Subterranean Biology 46: 97–127 (2023)
doi: 10.3897/subtbiol.46.108396
https://subtbiol.pensoft.net

RESEARCH ARTICLE

A peer-reviewed open-access journal
Subterranean Biology
Published by The International Society for Subterranean Biology

The first record of a stygobiotic form of *Garra rufa* (Heckel, 1843), sympatric with *Garra tashanensis* Mousavi-Sabet, Vatandoust, Fatemi & Eagderi, 2016 (Teleostei, Cyprinidae), in Iranian subterranean waters

Mohammad Javad Malek-Hosseini[1,2*], Jean-François Flot[3,4*], Yaser Fatemi[5], Hamid Babolimoakher[6], Matjaž Kuntner[1,2], Oleg A. Diripasko[7], Dušan Jelić[8], Nina G. Bogutskaya[9,10]

1 *Jovan Hadži Institute of Biology, Research Centre of the Slovenian, Academy of Sciences and Arts, SI-1000 Ljubljana, Slovenia* **2** *Department of Organisms and Ecosystems Research, National Institute of Biology, SI-1000 Ljubljana, Slovenia* **3** *Université libre de Bruxelles (ULB), Evolutionary Biology & Ecology, C.P. 160/12, Avenue F.D. Roosevelt 50, 1050 Brussels, Belgium* **4** *Interuniversity Institute of Bioinformatics in Brussels – (IB)², Brussels, Belgium* **5** *Department of Marine Biology, Faculty of Marine Sciences and Technology, University of Hormozgan, Bandar Abbas, Iran* **6** *Faculty of Geographical Sciences and Planning, University of Isfahan, Isfahan, Iran* **7** *Institute of Fisheries and Marine Ecology, Berdyansk, Ukraine* **8** *Croatian Institute for Biodiversity, Zagreb, Croatia* **9** *BIOTA J d.o.o, Dolga Gora, Slovenia* **10** *Naturhistorisches Museum Wien, Vienna, Austria*

Corresponding author: Mohammad Javad Malek-Hosseini (javad.malek@zrc-sazu.si; malekhosseini1365@gmail.com)

Academic editor: Maria Elina Bichuette | Received 21 June 2023 | Accepted 19 September 2023 | Published 17 October 2023

https://zoobank.org/0B922705-F502-424D-A8A4-5C04664127F8

Citation: Malek-Hosseini MJ, Flot J-F, Fatemi Y, Babolimoakher H, Kuntner M, Diripasko OA, Jelić D, Bogutskaya NG (2023) The first record of a stygobiotic form of *Garra rufa* (Heckel, 1843), sympatric with *Garra tashanensis* Mousavi-Sabet, Vatandoust, Fatemi & Eagderi, 2016 (Teleostei, Cyprinidae), in Iranian subterranean waters. Subterranean Biology 46: 97–127. https://doi.org/10.3897/subtbiol.46.108396

Abstract

We report the first finding of the stygobiotic form of the cyprinid fish *Garra rufa* (Heckel, 1843), discovered in a single locality in southwestern Iran, while the epigean form of the species is widely distributed in western Asia (Iran, Jordan, Lebanon, Turkey, and Syria). We also report a new locality for its hypogean congener, *Garra tashanensis*, about 5 km east of its type locality. The two species occur in syntopy in out-

* These authors contributed equally.

flows of the Tang-e-Ban, a seasonal karstic spring that only has flowing water during winter and spring, when fish individuals are washed from the cave to the surface. Identification of the investigated samples was confirmed by morphological analyses, COI distances, and a phylogenetic tree. These findings suggest the existence of a large karst aquifer in the Tashan area that harbours several cave species of fish, crustaceans, and gastropods and may have considerable conservation implications.

Keywords
Conservation, Iran, phylogeny, stygobionts, Tashan, Zagros

Introduction

Over 20 hotspots for subterranean biodiversity have been declared worldwide (Culver et al. 2021). These environments harbour a unique diversity of aquatic and terrestrial animals. Adaptations, both ecological and morphological, to the underground environment were the focus of many faunistic, evolutionary, and conservational studies (e.g., Dudich 1932; Pavan 1944; Ruffo 1957; Christiansen 1962, 2012; Sket 1985, 1999, 2004; Romero and Paulson 2001; Pipan and Culver 2012; Zagmajster et al. 2018; Borko et al. 2021) that revealed a continuum of levels (or a degree) of adaptations to underground environment.

For many species, both epigean (surface) and hypogean (subterranean) forms have been described that show variable morphological cave-related traits (Kruckenhauser et al. 2011; Pipan and Culver 2012; Kirchner et al. 2017, 2020, 2021; Bilandžija et al. 2018, 2020). These traits have been termed troglomorphisms by Christiansen (1962, 2012). Christiansen emphasised the lack of eyes and dark pigmentation but, presently, the term has been expanded to include any autapomorphy of exclusively subterranean species that may be directly related to the subterranean selective regime (Trajano and De Carvalho 2017; Culver and Pipan 2019). Troglomorphisms have been commonly separated into regressive and constructive traits (Wilkens 1988; Wilkens and Strecker 2017). Regressive traits are characterised by the loss of an organ or function, whereas constructive traits lead to an increase in the number of organs or functions, or an increase in their performance. The most prominent regressive traits in cave fishes are eye degradation and the overall reduction in pigmentation (Wilkens 1988; Jeffery 2001, 2005; Stemmer et al. 2015; Krishnan and Rohner 2016). Other morphological changes, with some related to behavioural differences, have evolved in cave fishes: for instance, the size and number of their cranial neuromasts are decreased. However, cave fishes display many other differences in morphological features (including anatomical and skeletal ones) that are not easy to interpret in terms of adaptation to subterranean habitat. In reviewing these issues, Jeffery (2001, 2005) and Yamamoto and Jeffery (2011) concluded that, in general, many regressive changes in cave fish seem to be related to loss of sight, whereas most constructive changes (although some regressive changes can be, at the same time, constructive in particular cases) seem to be related to

feeding and/or swimming behaviour, and there are a few presumably neutral changes that presently defy explanation.

To date, about 300 species of cave fishes (Proudlove 2023) have been described, and of these, 64 species are from the family Cyprinidae. In particular, eight cyprinid species of the genus *Garra* Hamilton, 1822 are known troglobionts/stygobionts from South-East and South-West Asia, the Middle East, the Arabian Peninsula, and Africa. Species of *Garra* are found in fast-flowing waters such as streams and rivers, but also in lakes, springs, and caves (Krupp and Schneider 1989; Mousavi-Sabet et al. 2016; Zamani-Faradonbe and Keivany 2021). Cyprinidae with more than 63 confirmed species is the most diverse family in Iranian inland freshwater (Jouladeh-Roudbar et al. 2020). In Iran, 11 *Garra* species are known from freshwater basins (Esmaeili et al. 2016, 2017; Zamani-Faradonbe and Keivany 2021). Three of them inhabit subterranean waters in the Zagros Mountains: *Garra lorestanensis* Mousavi-Sabet & Eagderi, 2016 and *G. typhlops* (Bruun & Kaiser, 1948) occur in sympatry in Loven cave and Tuveh spring (Vatandoust et al. 2019), also together with a species from the family Nemacheilidae, *Eidinemacheilus smithi* (Greenwood, 1976) (Malek-Hosseini et al. 2022); whereas, *G. tashanensis* Mousavi-Sabet, Vatandoust, Fatemi & Eagderi, 2016 is found in Tashan cave.

Garra rufa (Heckel, 1843) is known from at least Iran, Turkey, and Syria, but so far only by its epigean (surface) form. Studies published since 2014 have provided genetic and morphological evidence for recognising some of the former subspecies and local forms of the *Garra rufa* complex as separate species, while other new species in the species complex have been described (Hamidan et al. 2014; Sayyadzadeh et al. 2015; Esmaeili et al. 2016; Mousavi-Sabet and Eagderi 2016; Mousavi-Sabet et al. 2016; Zamani-Faradonbe et al. 2020a). As a result, the range of the species is presently limited to the Tigris–Euphrates system, as well as to rivers of the Persian Gulf Basin in Iran.

The literature reports a number of morphological features that separate *Garra rufa* from its congeners in Iran and adjacent areas, such as usually 8½ branched dorsal-fin rays; the breast, belly, and predorsal mid-dorsal line fully covered by scales; eye placed in posterior half of head; the snout blunt and the head trapezoidal in dorsal view; usually 9+8 caudal-fin rays; the mental (jugular) disc fully developed; two pairs of barbels; 20–24 total gill rakers on the first branchial arch; the eyes well-developed; and a well pigmented, brown and silvery, colour pattern of the body (Ghalenoei et al. 2010; Hamidan et al. 2014; Esmaeili et al. 2016; Keivany et al. 2016; Zamani-Faradonbe et al. 2020a, b).

Here, we report the discovery of *Garra* cave fishes in Tang-e-Ban spring, five kilometres east of Tashan cave in the Zagros Mountains of southwestern Iran. Using morphology as well as COI sequence data, we show that two *Garra* species are present in sympatry in this location: one of them is the cave-restricted species *G. tashanensis* (a new record for this species), whereas the other is a novel obligate groundwater form of *Garra rufa*, a species that has so far only been recorded in surface waters.

Material and methods

Terminology

While many definitions are used in ecological and evolutionary classifications of hypogean organisms (Barr 1968; Sket 2008; Trajano and de Carvalho 2017; Culver and Pipan 2019), the objects of this study can be clearly classified, following criteria from the mentioned publications, as follows: 1. Cave fish is a generic term for fish adapted to life in caves and other underground habitats (near-synonymous terms are subterranean fish, troglomorphic fish, troglobiont, stygobiont, phreatic fish, and hypogean fish); 2. stygobiont (stygobiotic) is used for aquatic species exclusively inhabit the subterranean domain, and are unable to complete any part of their life cycle outside of subterranean habitats (obligatory cavernicole), they reproduce underground, are highly modified, and show the most profound adaptations to life in darkness.

Studied locality

Tang-e-Ban Spring is a seasonal spring (Figs 1, 2) located at 30°50'54"N, 50°13'03"E, five kilometres east of Tashan Cave (the type locality of *Garra tashanensis*), close to Ablash Village, in Tashan district, Behbahan County, Khuzestan Province. Depending on the amount of precipitation, water flows through the spring from February to May, but the spring dries out completely in summer.

Sampling

Samples were collected using a small hand net. Some specimens were photographed alive. Anaesthesia was carried out using etheric clove oil (*Eugenia caryophyllata*) diluted in water. Samples were preserved in 96% ethanol. The voucher specimens have been deposited in the Natural History Museum, Khuzestan Province (**NHMKH**), Iran and public collection of the Natural History Museum in Vienna (**NMW**), Austria. The museum numbers are given below in Examined Material.

Molecular procedures

DNA was isolated from fin clips using DNA Multisample kit (Thermo Fisher Scientific). A fragment of the mitochondrial COI gene was amplified using the primer pair FishF1 (5'-TCAACCAACCACAAAGACATTGGCAC-3') and FishR1 (5'-TAGACTTCTGGGTGGCCAAAGAATCA-3') (Ward et al. 2005) for some samples, and the primer pair VF2_t1 (5'-TGTAAAACGACGGCCAGTCAACCAACCACAAAGACATTGGCAC-3') and FR1d_t1 (5'-CAGGAAACAGCTATGACACCTCAGGGTGTCCGAARAAYCARAA-3') for other samples. PCR reactions were made in a 35 µl final reaction volume containing: 21.8 µL of H_2O, 7.1 µL of 10X DreamTaq Green Buffer, 0.5 µL of dNTP mix (10 mM each), 3.2 µL of $MgCl_2$

Figure 1. Map of Iran showing the studied localities: 1 (black): Tang-e-Ban Spring; 2 (blue): Tashan Cave; 3 (red): Sarjowshar Spring; 4 (green): Maroon River, Mooger.

(25 mM); 1 µL of each primer (20 mM), 0.2 µL of DreamTaq Green DNA Polymerase (5 U/µL) and 0.2 µL of bovine serumalbumine. PCR was performed using the following protocols: for the FishF1/FishR1 primer pair, 94 °C for 10 min; 30 cycles at 94 °C for 1 min, 58.5 °C for 1 min, 72 °C for 1 min; and a final extension for 5 min at 72 °C; for the primer VF2_t1/ FR1d_t1 primer pair: 94 °C for 2 min; 35 cycles of 94 °C for 30 s, 52 °C for 40 s, and 72 °C for 1 min; with a final extension at 72 °C for 10 min. The PCR products were sequenced by Macrogen Europe (Amsterdam, the Netherlands). The final alignment was 649 bp in length.

Sequences (17 original ones) were assembled and checked using ChromasPro 2.1.3 (Technelysium, Tewantin, Australia). An additional 17 sequences from 15 taxa were obtained from GenBank (Suppl. material 1). Sequences were aligned using MEGA 11 (Kumar et al. 2018) (Suppl. material 2) and the same programme was used to find the best substitutional model for Bayesian and Maximum Likelihood analyses, as well as to estimate Kimura 2-parameter (K2P) pairwise distances (Kimura 1980) (Table 1). Data were curated using Mesquite version 3.7 (Maddison and Maddison 2018), then

Figure 2. Tang-e-Ban Spring in different seasons: January 2023, dry (**a**); April-May 2022 (**b–e**).

Bayesian inference of phylogenies was conducted using MrBayes v. 3.2.7a (Huelsenbeck and Ronquist 2001) using *Cyprinus carpio* Linnaeus, 1758 as an outgroup (20 million generations, four MCMC chains, sampling frequency of 1/1000). A relative burn-in was set to 25% and convergence was checked using Tracer 1.7 (Rambaut et al. 2018). Maximum likelihood phylogenetic trees with 1000 fast bootstrap replicates were obtained in IQ-TREE v2.1.3 (Minh et al. 2020). The HKY+G model of nucleotide substitution was used for both analytical methods.

Morphological analyses

Morphological analyses were based on a total of 32 absolute measurements, 45 relative measurements (ratios), 9 external body counts, and 7 axial skeleton counts (from radiographs). Measurements were made point to point using a digital caliper to the nearest 0.1 mm (only for specimens with SL>39 mm as measuring smaller fish produces significant error); counts are defined in Tables 2–5. The snout morphology and categorisation follow Nebeshwar and Vishwanath (2017). The terminology used for the external oral morphology and the gular disc (commonly referred to as mental disc or mental adhesive disc, e.g., in Hashemzadeh Segherloo et al. (2016)) followed Kottelat (2020). Measurements of the gular disc included disc length (taken as the distance between the anterior median margin of the torus and the posterior-most end of the labrum at midline); maximum mouth width (distance between lateral margins of the labelli); disc width (maximum width of the labrum); and pulvinus width (maximum width of the pulvinus).

In the description, the posterior two branched rays in the dorsal and anal fins, located on the last complex proximal pterygiophore of the fin, were symbolised as 1½ while "½" was omitted in statistical analyses. Ray counts for dorsal and anal fins were taken from radiographs. Counts and terminology of the axial skeleton, examined from radiographs, followed Naseka (1996). Total number of lateral-line scales were counted as lateral-line segments (defined by pores) as, in some phenotypes, scales are poorly developed or absent, while respective canal segments are present.

To detect separation between specimens, phenotypes, and species in the morphospace, we used both principal component analysis (PCA) and cluster analysis (CA). Statistical analyses were performed using Microsoft Excel, Statistica 12 (StatSoft), and PAST version 4.09 (Hammer et al. 2001). As measurements were only taken from specimens with SL > 39 mm (20 specimens in total), whereas counts were taken from all examined specimens (33 specimens in total), statistical analyses were performed on either morphometric and meristic characters together, or on meristic characters (i.e., counts) only.

Examined material

Identification codes used in molecular and statistical analyses are given in parentheses.

Garra rufa

Epigean *G. rufa*: NMW 100637, 9 specs (Gr1-9), SL 49.3–74.8 mm; Maroon River, Mooger 10 km to the northeast of Tang-e-Ban Spring, 20.04.2022, coll. Fatemi Y.

Hypogean phenotype of *G. rufa* (identified as such based on molecular data as shown below): 5 specs (F60-62, F64-65), SL 34.5–52.9 mm; Tang-e-Ban Spring, 20.04.2022, coll. Babolimoakher H.

***Garra tashanensis*, disc-bearing phenotype**

Tang-e-Ban Spring (identified as *G. tashanensis* based on molecular data as shown below): NMW 100638, 1 specs (F63), 43.3 mm; 20.04.2022, coll. Babolimoakher H. (NHMKH) 12 specs (F66-75, A, B), SL 33.1–45.9 mm; SL 33.1–45.9 mm; same date and collector.

Tashan Cave: (NHMKH) 6 specs (F9, F44-46, F48, Y), SL 22.5–42.2 mm, 17.03.2018, coll. Malek-Hosseini MJ & Fatemi Y.

Comparative material: NMW 53257 (10), 53238 (4) - syntypes of *Discognathus obtusus* Heckel, 1843; NMW 53240 (8) – lectotype and paralectotypes of *Discognathus rufus* Heckel, 1843.

Results

Genetic analyses

Bayesian phylogeny placed the troglomorphic specimens from Tang-e-Ban Spring in a clade with surface *G. rufa* from a stream in Sarjowshar village about 7 km to the southwest of Tang-e-ban and with other *G. rufa* sequences from GenBank (Fig. 3). This Tang-e-Ban form, identified as *G. rufa* based on its COI sequence, is referred to as "hypogean *G. rufa*" in morphological analyses below. Specimens from another stygobiotic species, also inhabiting Tang-e-Ban Spring, were grouped with *G. tashanensis* exemplars (Fig. 3). *G. rufa* formed a well-supported clade together with *G. amirhosseini* Esmaeili, Sayyadzadeh, Coad & Eagderi, 2016, *G. elegans* (Günther, 1868), *G. mondica* Sayyadzadeh, Esmaeili & Freyhof, 2015, *G. widdowsoni* (Trewavas, 1955) and *G. persica* Berg, 1914, as well as *G. barreimiae* Fowler & Steinitz, 1956, *G. ghorensis* Krupp, 1982, *G. jordanica* Hamidan, Geiger & Freyhof, 2014, and a group of *Garra* including Lorestan cave barbs (*G. typhlops* and *G. lorestanensis*) and *G. gymnothorax* (Berg, 1949). This large clade was found to be sister to *G. tashanensis* with 0.84 posterior probability and 85% ultrafast bootstrap support.

Average estimates of genetic divergence (K2P) in the COI barcode region among the studied *Garra* samples and specimens (Table 1) revealed that hypogean *Garra rufa* of Tang-e-Ban spring shows a maximum of 1.09 % of K2P distance compared with

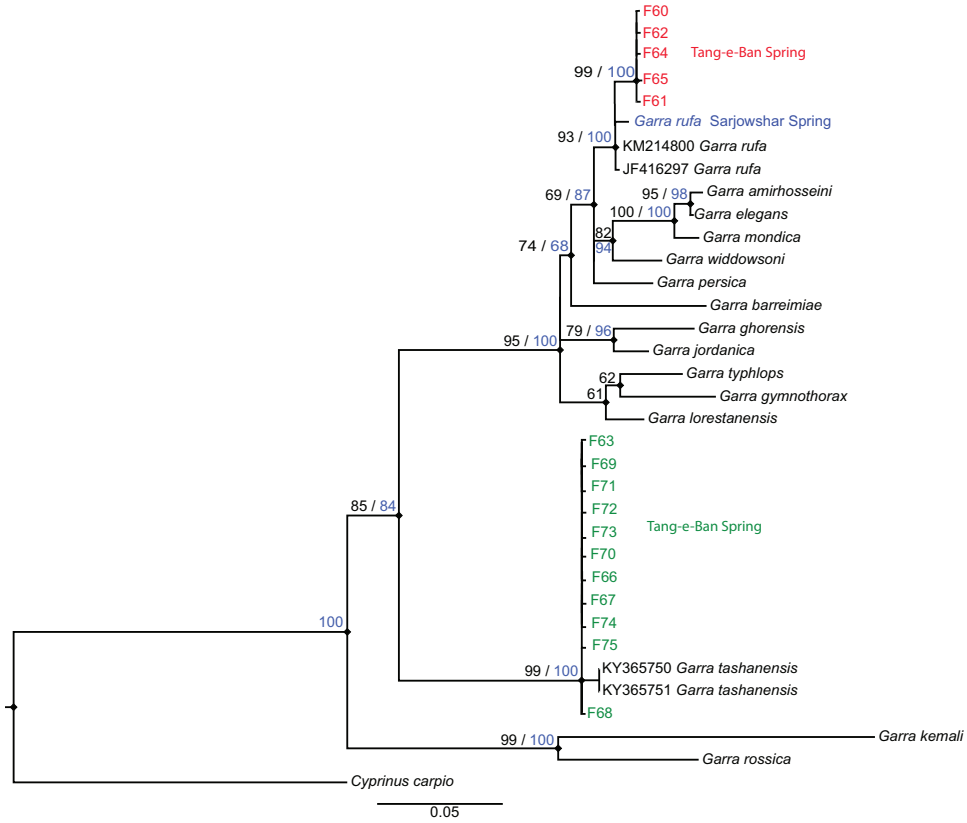

Figure 3. Phylogeny of the *Garra* lineage. The topology is from Bayesian inference analysis based on COI sequences. Blue values: posterior probabilities (Bayesian); black values: ultrafast bootstrap supports obtained by IQTREE (ML).

surface specimens from a stream in Sarjowshar village, and 0.31% with other *G. rufa* in the analyses. Analysed specimens of hypogean *G. tashanensis* from Tang-e-Ban Spring showed a maximum of 0.31% K2P distance among samples from this locality, and 0.78% K2P distance from sequences of Tashan cave individuals published by Mousavi-Sabet et al. (2016).

Morphological analyses

Garra rufa (Heckel, 1843)

Description of the cave sample (Tang-e-Ban Spring)

The general appearance of the body is shown in Figs 4, 5, morphometric data are given in Table 2 and counts are given in Table 3.

Table 1. Estimates of the average COI divergence (K2P distance) between examined *Garra* samples.* Tang-e-Ban Spring.

No.	Specimen name	1	2	3	4	5	6	7	8	9	10	11	12	13	14	15	16	17	18	19	20	21	22	23	24	25	26	27	28	29	30	31	32	33
1	KM214800 *Garra rufa*																																	
2	JF416297 *G. rufa*	0.31																																
3	*G. rufa* Sarjowshar Spring	0.46	0.77																															
4	F60 *G. rufa**	0.62	0.93	1.09																														
5	F61 *G. rufa**	0.62	0.93	1.09	0.00																													
6	F62 *G. rufa**	0.62	0.93	1.09	0.00	0.00																												
7	F64 *G. rufa**	0.62	0.93	1.09	0.00	0.00	0.00																											
8	F65 *G. rufa**	0.62	0.93	1.09	0.00	0.00	0.00	0.00																										
9	F63 *G. tashanensis**	10.30	10.30	10.49	11.04	11.04	11.04	11.04	11.04																									
10	F66 *G. tashanensis**	10.30	10.30	10.49	11.04	11.04	11.04	11.04	11.04	0.00																								
11	F67 *G. tashanensis**	10.24	10.24	10.43	10.98	10.98	10.98	10.98	10.98	0.00	0.00																							
12	F68 *G. tashanensis**	10.12	10.12	10.30	10.85	10.85	10.85	10.85	10.85	0.15	0.15	0.16																						
13	F69 *G. tashanensis**	10.30	10.30	10.49	11.04	11.04	11.04	11.04	11.04	0.00	0.00	0.00	0.15																					
14	F70 *G. tashanensis**	10.30	10.30	10.49	11.04	11.04	11.04	11.04	11.04	0.00	0.00	0.00	0.15	0.00																				
15	F71 *G. tashanensis**	10.30	10.30	10.49	11.04	11.04	11.04	11.04	11.04	0.00	0.00	0.00	0.15	0.00	0.00																			
16	F72 *G. tashanensis**	10.30	10.30	10.49	11.04	11.04	11.04	11.04	11.04	0.00	0.00	0.00	0.15	0.00	0.00	0.00																		
17	F73 *G. tashanensis**	10.30	10.30	10.49	11.04	11.04	11.04	11.04	11.04	0.00	0.00	0.00	0.15	0.00	0.00	0.00	0.00																	
18	F74 *G. tashanensis**	9.84	10.03	10.03	10.61	10.61	10.61	10.61	10.61	0.00	0.00	0.00	0.16	0.00	0.00	0.00	0.00	0.00																
19	F75 *G. tashanensis**	10.49	10.49	10.67	11.22	11.22	11.22	11.22	11.22	0.15	0.15	0.16	0.31	0.15	0.15	0.15	0.15	0.15	0.16															
20	KY365750 *G. tashanensis*	10.34	10.15	10.52	11.07	11.07	11.07	11.07	11.07	0.62	0.62	0.63	0.78	0.62	0.62	0.62	0.62	0.62	0.65	0.78														
21	KY365751 *G. tashanensis*	10.34	10.15	10.52	11.07	11.07	11.07	11.07	11.07	0.62	0.62	0.63	0.78	0.62	0.62	0.62	0.62	0.62	0.65	0.78	0.00													
22	*G. amirhosseini*	4.46	4.46	4.63	5.12	5.12	5.12	5.12	5.12	10.85	10.85	10.80	10.67	10.85	10.85	10.85	10.85	10.85	10.61	11.04	10.89	10.89												
23	KM214783 *G. barreimiae*	6.14	6.14	5.97	6.49	6.49	6.49	6.49	6.49	12.30	12.30	12.30	12.11	12.30	12.30	12.30	12.30	12.30	12.11	12.49	12.54	12.54	7.73											
24	*G. elegans*	4.30	4.30	4.46	4.96	4.96	4.96	4.96	4.96	11.04	11.04	10.99	10.86	11.04	11.04	11.04	11.04	11.04	10.80	11.23	11.08	11.08	0.46	7.55										
25	*G. ghorensis*	5.75	5.75	6.26	6.09	6.09	6.09	6.09	6.09	9.59	9.59	9.59	9.41	9.59	9.59	9.59	9.59	9.59	9.47	9.78	10.00	10.00	7.14	8.33	6.96									
26	KX570881 *G. gymnothorax*	6.23	6.40	6.40	6.58	6.58	6.58	6.58	6.58	12.55	12.55	12.55	12.35	12.55	12.55	12.55	12.55	12.55	12.42	12.74	12.59	12.59	6.94	8.51	6.41	8.22								
27	*G. jordanica*	4.13	4.13	4.63	4.79	4.79	4.79	4.79	4.79	10.67	10.67	10.80	10.48	10.67	10.67	10.67	10.67	10.67	10.60	10.85	10.70	10.70	6.13	6.84	5.96	3.89	6.58							
28	*G. kemali*	15.68	15.47	15.27	15.68	15.68	15.68	15.68	15.68	14.82	14.82	15.01	14.61	14.82	14.82	14.82	14.82	14.82	15.62	15.02	14.64	14.64	16.09	17.96	16.51	17.82	16.71	17.14						
29	KM214776 *G. lorestanensis*	4.46	4.46	4.63	4.46	4.46	4.46	4.46	4.46	9.77	9.77	9.88	9.59	9.77	9.77	9.77	9.77	9.77	9.85	9.95	9.80	9.80	6.47	7.37	6.30	6.62	4.66	5.46	13.23					
30	*G. mondica*	4.64	4.64	4.83	5.41	5.41	5.41	5.41	5.41	10.84	10.84	10.84	10.63	10.84	10.84	10.84	10.84	10.84	10.84	11.06	10.86	10.86	2.00	7.52	1.45	7.00	5.62	6.19	17.11	6.59				
31	*G. persica*	3.01	3.01	3.49	3.66	3.66	3.66	3.66	3.66	10.54	10.54	9.89	10.35	10.54	10.54	10.54	10.54	10.54	9.47	10.72	10.57	10.57	4.65	5.97	4.81	6.27	6.58	5.98	15.76	5.31	4.83			
32	*G. rossica*	13.75	13.75	13.94	13.75	13.75	13.75	13.75	13.75	14.07	14.07	14.04	13.87	14.07	14.07	14.07	14.07	14.07	14.38	14.26	14.11	14.11	14.14	15.81	14.72	14.10	15.85	14.72	11.46	13.36	14.67	13.43		
33	KM214717 *G. typhlops*	5.29	5.29	5.13	5.29	5.29	5.29	5.29	5.29	10.84	10.84	10.97	10.66	10.84	10.84	10.84	10.84	10.84	10.79	11.03	10.88	10.88	6.65	7.56	6.82	6.28	5.01	5.63	13.25	3.64	6.99	5.82	12.20	
34	*G. widdowsoni*	3.32	3.32	3.80	3.64	3.64	3.64	3.64	3.64	10.85	10.85	10.80	10.67	10.85	10.85	10.85	10.85	10.85	10.80	11.04	10.89	10.89	4.30	7.01	4.13	6.96	7.11	5.62	16.30	5.29	4.07	4.48	15.31	6.47

Table 2. Morphometrics of examined *Garra rufa*.

	Hypogean sample, Tang-e-Ban			Epigean sample, Maroon River; n=9			
Sample label	**F60**	**F62**	**F64**	**min**	**max**	**mean**	**SD**
SL, mm	41.9	52.9	40.7	49.3	74.8	61.8	8.0
Maximum body depth (% SL)	20.1	20.3	20.2	19.8	25.5	22.5	1.7
Depth of caudal peduncle (% SL)	10.1	11.1	10.2	12.1	13.9	12.8	0.6
Depth of caudal peduncle (% length of caudal peduncle)	59.1	53.0	54.2	71.4	82.2	78.4	4.2
Body width (% SL)	15.3	15.3	15.4	14.1	17.4	15.8	1.1
Caudal-peduncle width (% SL)	8.4	8.6	8.6	7.0	9.7	8.4	0.8
Predorsal length (% SL)	51.4	51.3	51.6	45.9	50.0	48.0	1.3
Postdorsal length (% SL)	40.8	42.8	45.0	31.8	39.1	36.8	2.2
Prepelvic length (% SL)	52.9	56.2	56.6	49.8	55.2	53.4	1.8
Preanal length (% SL)	73.4	74.9	75.5	76.3	81.6	79.6	1.5
Pectoral – pelvic-fin origin length (% SL)	29.9	31.3	33.3	29.1	32.5	31.0	1.3
Pelvic – anal-fin origin length (% SL)	20.6	19.9	20.9	25.9	29.1	27.2	1.0
Caudal-peduncle length (% SL)	18.1	20.8	18.7	15.0	17.4	16.4	1.2
Dorsal-fin base length (% SL)	12.5	13.2	13.3	15.4	18.1	16.1	1.6
Dorsal-fin depth (% SL)	18.3	20.5	20.7	15.8	22.1	19.4	2.4
Anal-fin base length (% SL)	8.4	8.7	8.8	7.1	9.0	8.0	0.6
Anal-fin depth (% SL)	18.3	17.7	17.9	14.8	18.4	16.7	1.3
Pectoral-fin length (% SL)	19.7	20.9	19.1	20.8	24.3	22.9	1.3
Pelvic-fin length (% SL)	17.6	18.5	16.6	17.3	20.3	18.7	1.1
Head length (% SL)	22.9	23.5	24.0	21.9	24.1	23.3	0.8
Head length (% body depth)	113.7	116.0	118.7	92.6	121.4	104.4	9.0
Head depth at nape (% SL)	16.1	16.2	16.3	15.8	17.8	16.5	0.7
Head depth at nape (% HL)	70.2	68.9	67.9	67.1	75.9	71.0	3.1
Anus – anal-fin origin distance (% pelvic – anal-fin origin length)	32.3	28.3	30.4	24.4	31.6	27.8	2.3
Maximum head width (% SL)	17.3	17.0	17.2	16.3	18.4	17.5	0.6
Maximum head width (% HL)	75.9	72.5	71.4	68.9	78.8	75.3	3.1
Anterior barbel length (% SL)	4.3	4.2	4.8	2.8	5.4	3.8	0.8
Anterior barbel length (% HL)	52.2	40.2	51.2	30.0	42.8	35.2	4.5
Anterior barbel length (% internasal width)	82.7	66.6	66.7	38.5	68.9	50.1	9.4
Posterior barbel length (% SL)	5.5	5.2	5.2	2.1	6.3	4.2	1.2
Posterior barbel length (% HL)	19.7	22.0	21.7	9.4	27.3	17.8	5.1
Internasal width (% SL)	7.6	6.3	7.2	7.2	7.8	7.5	0.2
Internasal width (% HL)	33.2	27.0	29.8	29.9	34.9	32.1	1.6
Maximum mouth width (% HL)	42.5	40.4	39.8	40.5	48.5	45.3	3.1
Maximum mouth width (% SL)	9.7	9.5	9.6	9.0	11.5	10.6	0.9
Mouth cleft transverse length (% SL)	6.9	7.3	7.3	6.7	10.1	8.3	1.1
Mouth cleft transverse length (% HL)	30.1	30.9	30.5	30.6	42.4	35.4	4.0
Mouth cleft transverse length (% internasal width)	90.6	114.6	102.4	88.7	132.6	110.6	14.1
Disc width (% HL)	35.3	33.8	33.4	33.0	43.0	37.8	3.6
Pulvinus width (% HL)	19.7	22.0	21.7	9.4	27.3	17.8	5.1
Disk length (% disk width)	94.8	100.7	100.6	71.3	91.8	80.7	7.3
Disk length (% HL)	33.1	34.0	33.6	26.4	35.7	30.4	2.8
Width between ventral extremities of gill slits (% maximum head width)	53.9	54.1	54.0	63.1	74.8	67.6	3.8
Width between ventral extremities of gill slits (% HL)	40.9	39.2	38.6	45.3	56.9	50.9	3.5
Width between dorsal extremities of gill slits (% maximum head width)	80.4	85.9	88.3	80.8	92.2	87.7	4.4
Width between dorsal extremities of gill slits (% HL)	61.0	62.3	63.1	61.6	72.1	65.9	3.8

Longest examined specimen (F62) 52.9 mm SL (Fig. 4c). Body elongated, moderately thick, more compressed in region of caudal peduncle. Dorsal head profile rising gently, flat or slightly convex, more or less continuous with dorsal body profile to nape or about middle between nape and dorsal-fin origin. Ventral profile more or less straight to anal-fin origin. Head moderately large and markedly depressed, with slightly convex or flat interorbital distance; depth at nape considerably less than head length; width at nape exceeding head depth at nape. Snout blunt and smooth; neither

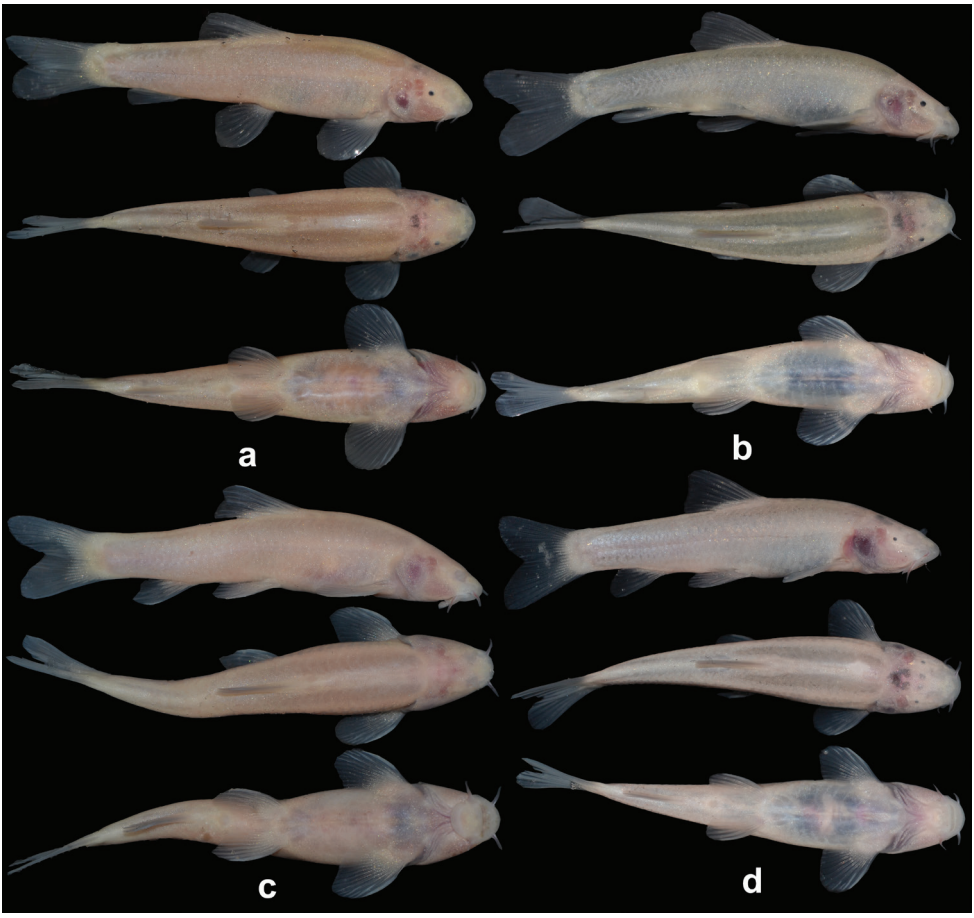

Figure 4. Hypogean *Garra rufa*, Tang-e-Ban Spring, 20.04.2022, before preservation (just anesthetized), right lateral, dorsal and ventral views: F60, SL 41.9 mm (**a**); F61, SL 35.2 mm (**b**); F62, SL 52.9 mm (**c**); and F64, SL 40.7 mm (**d**).

Table 3. Counts in examined *Garra rufa*.

	Hypogean sample, Tang-e-Ban					Epigean sample, Maroon River; n=9			
Sample label	**F60**	**F61**	**F62**	**F64**	**F65**	**min**	**max**	**mean**	**SD**
Number of unbranched dorsal-fin rays	3	3	3	3	4	3	4	3.8	0.4
Number of branched dorsal-fin rays (without 1/2)	7	7	7	7	7	8	8	8.0	0.0
Number of unbranched anal-fin rays	3	3	3	3	3	3	3	3.0	0.0
Number of branched anal-fin rays (without 1/2)	5	5	5	5	5	5	5	5.0	0.0
Number of simple pectoral-fin rays	1	1	1	1	1	1	1	1.0	0.0
Number of branched pectoral-fin rays	13	13	13	12	12	12	13	12.6	0.5
Number of simple pelvic-fin rays	1	1	1	1	1	1	1	1.0	0.0
Number of branched pelvic-fin rays	7	7	8	7	8	7	8	7.4	0.5
Number of predorsal vertebrae	11	11	11	11	11	10	11	10.3	0.5
Number of abdominal vertebrae	19	20	20	19	20	20	20	20.0	0.0
Number of pre-anal caudal vertebrae	2	2	2	3	2	3	5	3.8	0.7
Number of post-anal caudal vertebrae	13	14	14	13	13	11	12	11.6	0.5
Number of caudal vertebrae	15	16	16	16	15	14	16	15.3	0.7
Total vertebrae	34	36	36	35	35	34	36	35.2	0.7
Vertebrae between first pterygiophores of dorsal and anal fins	10	11	11	11	11	12	14	13.2	0.8
Number of total lateral-line scales	35	35	34	33	34	33	36	34.9	0.9

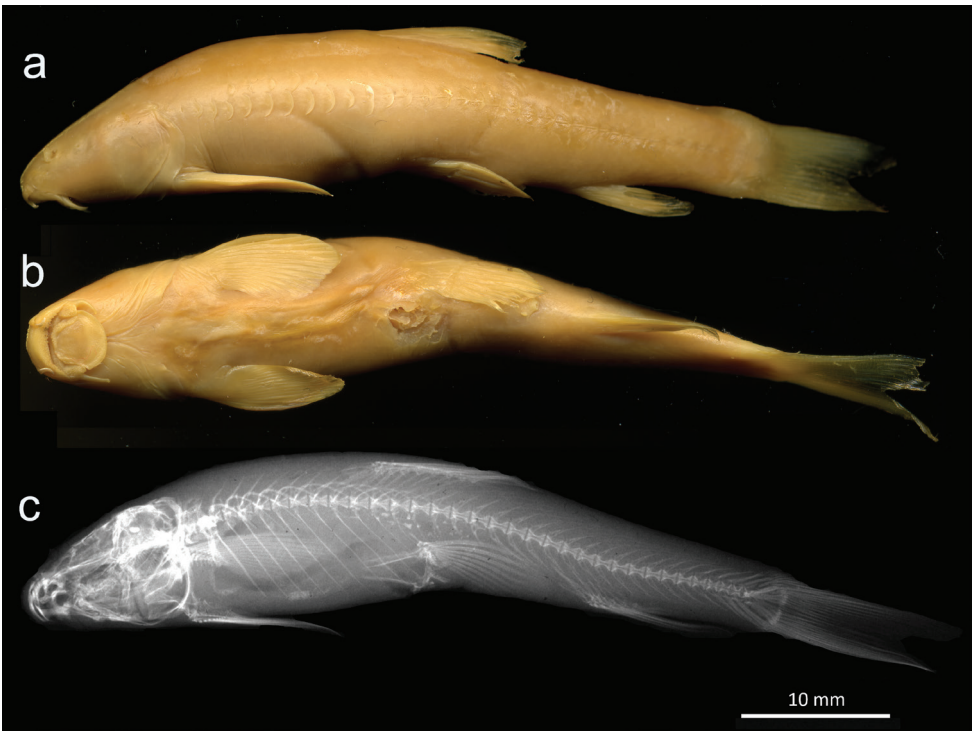

Figure 5. Hypogean *Garra rufa*, Tang-e-Ban Spring, 20.04.2022, preserved specimen (F62, SL 52.9 mm): left lateral view (**a**), ventral view (**b**) and radiograph (**c**). Radiograph showing distinguishing characters: 7½ branched dorsal-fin, 2 pre-anal caudal vertebrae, 14 post-anal caudal vertebrae, and 11 vertebrae between first pterygiophores of dorsal and anal fins.

transverse groove nor transverse lobe developed. Anterior extremity of ethmoid field (proboscis) not elevated from depressed rostral surface. Tubercles absent.

Eye variably reduced from almost "normal" eye to complete lack of externally visible structures; reduction asymmetrical (in 4 specimens), as follows, by specimens (left / right side of head). F60: eye pigmented; fossa small / eye pigmented; fossa small; F61 (Fig. 4b): eye slightly pigmented; fossa very small / eye pigmented; fossa comparatively large; F62 (Fig. 4c): no pigmented eye; fossa very small / no pigmented eye; no fossa; F 64 (Fig. 4d): eye pigmented; fossa very small / eye pigmented; fossa very small; F 65: eye pigmented; no fossa / eye pigmented; fossa small.

Gular disc well-developed, with free lateral and posterior margins, roundish, its width about equal to length; no considerable variability of its size and shape found in examined specimens. Mouth inferior, mouth cleft clearly straight. Papillae on torus, labellum and labrum. Rostral cap well-developed, fimbriate, papillate on ventral surface. Upper jaw almost or completely covered by rostral cap. Barbels in two pairs; anterior barbel well-developed, long; posterior barbel at corner of mouth, variably longer than rostral barbel.

Dorsal fin with 3 in 4 specimens and 4 in one specimen simple and 7½ branched rays; outer dorsal-fin margin about straight or slightly concave; origin at about middle of body, inserted anterior to vertical from pelvic-fin origin; first branched ray long-

est. Pectoral fin with 1 simple and 12–13 branched rays, depth less than head length. Pelvic fin with 1 simple and 7–8 branched rays, origin closer to anal-fin origin than to pectoral-fin origin, inserted below second or third branched dorsal-fin ray. Anal fin with 3 simple and 5½ branched rays; first branched ray longest; distal margin slightly to markedly concave; origin closer to caudal-fin base than to pelvic-fin origin. Distance between anus and anal-fin origin about equal to one third of pectoral – pelvic-fin origin length. Caudal fin forked with Caudal fin forked with 2+17(9+8) principal rays.

Body variably naked. Most scales lacking except for complete or almost complete lateral line with 33–35 total scales (Fig. 5). Besides lateral-line scales, few scattered or more numerous overlapping scales present on sides of trunk and caudal peduncle in 4 specimens out of 5 examined: 9–19 above lateral line and 2–12 below lateral line. Lateral-line scales comparatively well ossified, visible without staining with Alizarin Red S along most lateral line except for terminal section where lateral canal still well seen by normally developed sensory pores. Cephalic sensory canals complete, fully developed, non-interrupted.

Total vertebrae 34(1), 35(2) or 36(2); abdominal vertebrae 19(2) or 20(3); predorsal abdominal vertebrae 11; caudal vertebrae 15 (including 2 pre-anal and 13 post-anal caudal vertebrae) or 16 (2+14 in 2 specimens and 3+13 in one); and 10(1) or 11(4) vertebrae between first pterygiophores of dorsal and anal fins.

Body and fins unpigmented; body of live specimens (Fig. 4) pinkish because of blood vessels seen through the semi-transparent skin. In preserved specimens, body turns yellowish-white.

Comparison with epigean sample of *Garra rufa*

The sample examined from Maroon River did not depart from "typical" *G. rufa* morphology. We did not specifically analyse morphometric differences of the Maroon sample from *G. rufa* in other Iranian localities. The morphometric parameters of this species are age-and-size dependent and may be also influenced by habitat parameters (see, e.g., Zamani-Faradonbe et al. 2020a, b, Zamani-Faradonbe and Keyvani 2021). However, the diagnostic features of the species (such as most count characters and the gular disc shape) were shared by the Maroon sample and the examined type material of *G. rufa* and *G. obtusa* (a synonym of *G. rufa*). They are as follows: breast, belly, predorsal and mid-dorsal line fully covered by scales; lateral line complete, with 33–36 total lateral-line scales; snout blunt and head trapezoidal in dorsal view; jugular disc fully developed, wider than long; two pairs of barbels; eyes well-developed; brown and silvery colour pattern; 9+8 caudal-fin rays; commonly 4 unbranched dorsal-fin rays; 8½ branched dorsal-fin rays; 34–36 total vertebrae; 20 abdominal vertebrae; 10–11 predorsal abdominal vertebrae; 14–16 caudal vertebrae (including 3–5 pre-anal and 11–12 post-anal caudal vertebrae); and 12–14 vertebrae between first pterygiophores of dorsal and anal fins (Tables 2, 3).

A comparison of the examined epigean and hypogean samples revealed some clear differences between them. Although some morphometric differences may be due to the fact that the hypogean specimens (SL of morphometrically examined specimens

was 40.7–52.9 mm) were smaller than the epigean ones (SL 49.3–74.8 mm), the differences still deserve attention as they corroborate differences in some meristic characters. Among the morphometric parameters, the most statistically significant differences (the results of the statistical analyses are presented below) were found in the following relative measurements (Table 2): depth of caudal peduncle (10–11% SL and 53–59% of caudal peduncle length for hypogean specimens vs. 12–14 and 71–82 for epigean ones); caudal peduncle length (18–21% SL vs. 15–17); predorsal length (51–52% SL vs. 46–50); postdorsal length (41–45% SL vs. 32–39); pre-anal length (73–75% SL vs. 76–82); pelvic to anal-fin origin length (20–21% SL vs. 26–29); dorsal-fin base length (13% SL vs. 15–18); distance between ventral extremities of gill slips (39–41% HL vs. 45–57); gular disc length (95–101% of disc width vs. 71–91), meaning gular disc about as long as wide in hypogean sample (Fig. 5) in contrast to markedly wider than long in the epigean form (Fig. 6). Relative head length and most relative measurements on the head (Table 2) were similar in the two samples except for the mentioned gular disc parameters and the distance between the ventral extremities of the gill slips.

Among the examined morphometric characters, the most prominent differences were 7½ branched dorsal-fin rays in the hypogean sample (vs. 8½ in the epigean fish); 2 or 3 (in one specimen only) pre-anal caudal vertebrae (vs. 3–5, commonly 4); 13–14 post-anal caudal vertebrae (vs. 11–12); and 10–11 vertebrae between first pterygiophores of dorsal and anal fins (vs. 12–14) (Tables 2, 3). These characters entail some morphometric difference (difference in external characters) described above, namely, a shorter base of the dorsal fin when compared to the epigean specimens with 8½ branched dorsal-fin rays, and, as a result, different predorsal and postdorsal distances. The difference in the structure of the caudal vertebral region (2+[13–14] vs. 4+[11-12]) determines not only the difference in the number of vertebrae between first pterygiophores of dorsal and anal fins (pre-anal caudal subregion is shorter and the post-anal subregion is longer in the hypogean fish) but also the position of the anal fish externally expressed through, e.g., pre-anal distance and length of caudal peduncle.

The hypogean and epigean samples were clustered in distinct groups in the CA (Fig. 7) and formed well-separated groups in the morphospace using PCA using the combination of morphometric and meristic characters, as well as when using only meristic characters (Figs 7a, 8a). Interestingly, that in the CA, the hypogean *G. rufa* sample

Figure 6. Epigean (surface) *Garra rufa*, Maroon River, Mooger, 10 km to the northeast of Tang-e-Ban Spring, 20.04.2022.

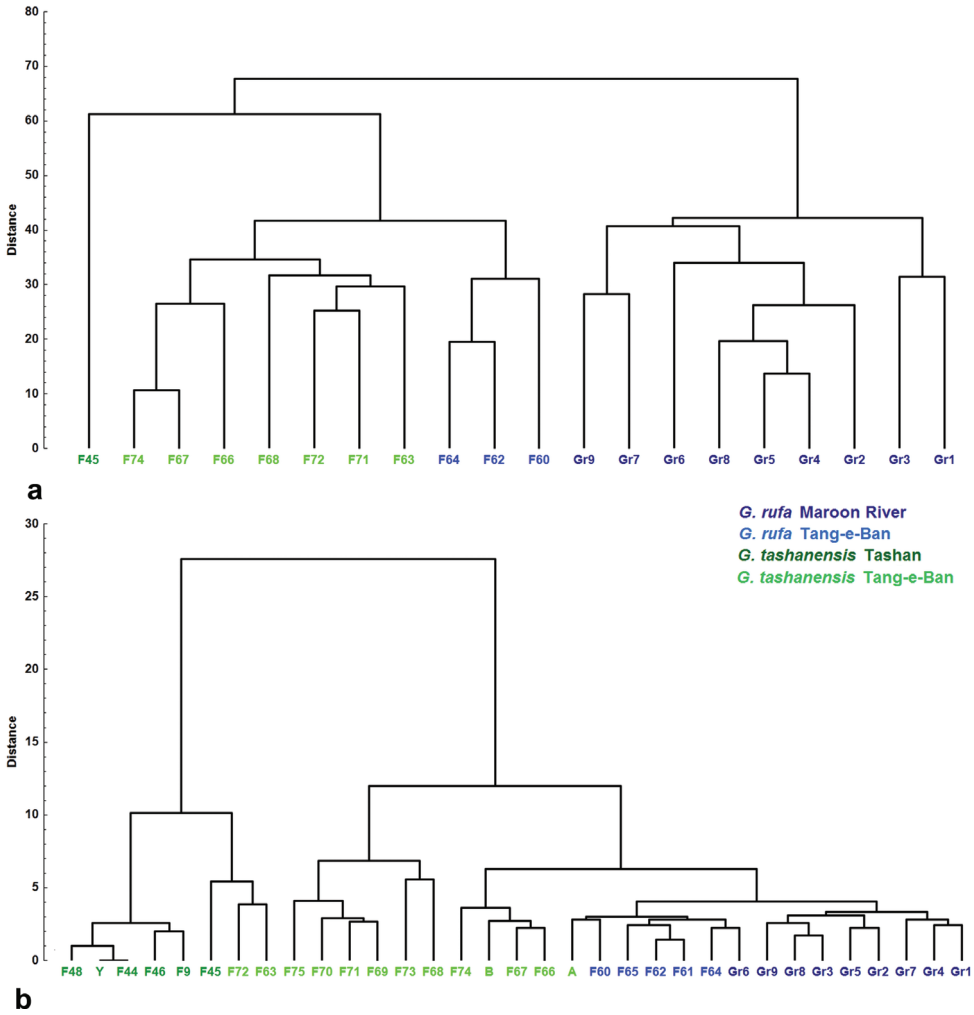

Figure 7. Results of CA: using morphometric and meristic characters (total of 20 specimens) (**a**); using only meristic characters (total of 33 specimens) (**b**).

clustered together with the syntopic *G. tashanensis*, not with epigean *G. rufa*, occurring nearby. When only meristic characters were used, the two groups were much closer in PCA (Fig. 7b) and, in CA (Fig. 8b), and even clustered together with one specimen of epigean *G. rufa* and one specimen of Tang-e-Ban *G. tashanensis.*

Garra tashanensis Mousavi-Sabet, Vatandoust, Fatemi & Eagderi, 2016

Description of the Tang-e-Ban Spring disc-bearing form

The general appearance of the body is shown in Figs 9–11, morphometric data are given in Tables 4, 5.

Table 4. Morphometrics of examined *Garra tashanensis* (SL>39.0 mm).

	Disc-bearing phenotype, Tang-e-Ban, 7 specs.									Disc-bearing phenotype, Tashan Cave (type-locality)
	F63	**F66**	**F67**	**F68**	**F71**	**F72**	**F74**	**mean**	**SD**	**F45**
SL, mm	43.3	45.9	41.4	39.5	41.5	41.4	40.1	41.9	2.1	42.2
Maximum body depth (% SL)	18.2	22.0	18.7	21.6	18.4	19.9	19.8	19.8	1.5	24.3
Depth of caudal peduncle (% SL)	11.2	13.3	11.9	12.1	11.3	12.5	11.8	12.0	0.7	12.0
Depth of caudal peduncle (% length of caudal peduncle)	55.0	64.2	61.0	69.2	55.1	66.6	59.5	61.5	5.5	79.7
Body width (% SL)	16.0	16.5	15.2	16.4	14.3	16.1	15.7	15.8	0.8	20.1
Caudal-peduncle width (% SL)	8.1	8.3	7.7	7.3	7.7	7.5	8.0	7.8	0.4	8.6
Predorsal length (% SL)	56.7	55.6	53.2	56.2	54.9	53.4	53.1	54.7	1.5	51.5
Postdorsal length (% SL)	37.6	40.3	36.9	37.7	35.4	37.9	38.5	37.8	1.5	36.7
Prepelvic length (% SL)	58.2	59.2	56.2	56.9	56.3	57.4	56.5	57.2	1.1	56.0
Preanal length (% SL)	80.4	82.0	77.4	78.0	77.6	78.6	78.2	78.9	1.7	76.6
Pectoral – pelvic-fin origin length (% SL)	32.6	36.8	34.3	33.5	33.1	35.1	33.8	34.2	1.4	31.6
Pelvic – anal-fin origin length (% SL)	21.8	21.9	19.2	20.9	19.3	17.7	19.6	20.1	1.5	20.5
Caudal-peduncle length (% SL)	20.3	20.8	19.5	17.5	20.4	18.8	19.8	19.6	1.1	15.0
Dorsal-fin base length (% SL)	10.5	10.3	10.6	10.7	12.2	9.9	9.8	10.6	0.8	12.3
Dorsal-fin depth (% SL)	18.5	19.3	17.3	18.7	16.8	17.4	18.4	18.1	0.9	20.9
Anal-fin base length (% SL)	7.9	8.1	7.7	7.5	7.4	8.1	7.7	7.8	0.3	6.8
Anal-fin depth (% SL)	16.6	17.0	15.8	15.2	14.9	17.0	16.2	16.1	0.8	14.8
Pectoral-fin length (% SL)	16.8	18.2	18.9	16.7	16.8	17.6	18.6	17.7	0.9	20.9
Pelvic-fin length (% SL)	14.8	14.6	14.9	15.3	14.3	14.4	16.1	14.9	0.6	16.7
Head length (% SL)	25.3	24.7	24.9	25.3	24.5	24.7	25.5	25.0	0.4	28.0
Head length (% body depth)	138.6	112.2	133.0	116.9	133.3	124.2	129.0	126.7	9.5	115.3
Head depth at nape (% SL)	13.6	14.8	13.9	15.1	14.2	14.6	14.1	14.3	0.5	18.2
Head depth at nape (% HL)	53.6	59.9	55.7	59.9	57.9	59.0	55.3	57.3	2.5	65.1
Anus – anal-fin origin distance (% pelvic – anal-fin origin length)	30.1	32.8	27.9	23.3	32.8	30.2	30.0	29.6	3.3	18.9
Maximum head width (% SL)	18.4	19.0	19.3	20.0	19.4	18.9	19.4	19.2	0.5	21.7
Maximum head width (% HL)	72.8	76.9	77.3	79.0	79.3	76.5	76.1	76.8	2.2	77.6
Anterior barbel length (% SL)	5.6	5.6	5.5	6.2	5.5	5.7	5.3	5.6	0.3	7.2
Anterior barbel length (% HL)	45.7	44.1	48.4	50.2	49.2	48.9	48.9	47.9	2.2	42.3
Anterior barbel length (% internasal width)	72.7	83.2	83.1	74.9	18.4	19.9	79.6	77.1	4.8	98.7
Posterior barbel length (% SL)	8.2	6.7	6.6	7.3	6.8	6.7	6.4	6.9	0.6	4.0
Posterior barbel length (% HL)	32.3	27.2	26.4	28.9	27.7	27.0	25.1	27.8	2.3	14.1
Internasal width (% SL)	7.7	6.7	6.6	8.3	7.6	7.7	6.7	7.3	0.7	7.3
Internasal width (% HL)	30.4	27.3	26.4	32.8	31.1	31.3	26.3	29.4	2.7	26.0
Maximum mouth width (% HL)	41.8	45.1	39.2	40.0	37.4	40.0	41.6	40.7	2.4	50.8
Maximum mouth width (% SL)	10.6	11.1	9.8	10.1	9.2	9.9	10.6	10.2	0.7	14.2
Mouth cleft transverse length (% SL)	7.6	7.9	7.1	7.4	6.9	7.2	7.5	7.4	0.3	8.4
Mouth cleft transverse length (% HL)	30.0	31.9	28.6	29.4	28.1	29.1	29.4	29.5	1.2	30.1
Mouth cleft transverse length (% internasal width)	98.5	116.8	108.5	89.6	90.5	92.8	111.9	101.2	11.1	116.0
Disc width (% HL)	32.2	34.6	30.4	30.4	29.4	30.9	32.0	31.4	1.7	43.7
Pulvinus width (% HL)	32.3	27.2	26.4	28.9	27.7	27.0	25.1	27.8	2.3	14.1
Disk length (% disk width)	92.6	91.6	93.9	90.8	91.0	99.1	91.4	92.9	2.9	70.8
Disk length (% HL)	29.9	31.7	28.6	27.6	26.7	30.6	29.2	29.2	1.7	31.0
Width between ventral extremities of gill slits (% maximum head width)	43.4	49.4	43.5	34.4	45.7	52.6	46.0	45.0	5.7	36.1
Width between ventral extremities of gill slits (% HL)	31.6	38.0	33.6	27.2	36.2	40.2	35.0	34.5	4.3	28.0
Width between dorsal extremities of gill slits (% maximum head width)	68.9	75.7	71.4	66.4	72.6	73.4	70.6	71.3	3.0	70.8
Width between dorsal extremities of gill slits (% HL)	50.1	58.2	55.2	52.5	57.5	56.2	53.7	54.8	2.9	54.9

Longest examined specimen 45.9 mm SL (F66, Fig. 9b). Body shape considerably variable (Figs 9, 10a–c). Head slightly to markedly (Figs 9a, 10c) depressed, its transition to back with nuchal hump especially prominent in specimens with depressed head.

Table 5. Counts in examined *Garra tashanensis*.

	Disc-bearing phenotype, Tang-e-Ban Spring, 13 specs (SL 33.1-45.9 mm)				Disc-bearing phenotype, Tashan Cave (type-locality)					
	min	**max**	**mean**	**SD**	**F9**	**F45**	**F44**	**F46**	**F48**	**Y**
SL, mm	33.1	45.9	38.8	4.0	34.8	42.2	26	25.1	24.5	22.5
Number of unbranched dorsal-fin rays	2.0	3.0	2.2	0.4	3	3	3	3	3	3
Number of branched dorsal-fin rays (without 1/2)	7.0	7.0	7.0	0.0	7	7	7	7	7	7
Number of unbranched anal-fin rays	2.0	2.0	2.0	0.0	2	2	2	2	2	2
Number of branched anal-fin rays (without 1/2)	5.0	5.0	5.0	0.0	5	5	5	5	5	5
Number of simple pectoral-fin rays	1.0	1.0	1.0	0.0	1	1	1	1	1	1
Number of branched pectoral-fin rays	11.0	14.0	12.1	0.9	14	13	13	14	14	13
Number of simple pelvic-fin rays	1.0	1.0	1.0	0.0	1	1	1	1	1	1
Number of branched pelvic-fin rays	6.0	8.0	7.1	0.7	7	7	7	7	7	7
Number of predorsal vertebrae	11.0	13.0	11.7	0.6	10	10	10	10	10	10
Number of abdominal vertebrae	18.0	19.0	18.5	0.5	17	18	18	18	18	18
Number of pre-anal caudal vertebrae	3.0	4.0	3.1	0.3	3	2	3	2	3	3
Number of post-anal caudal vertebrae	12.0	14.0	12.8	0.7	12	13	13	13	13	13
Number of caudal vertebrae	15.0	17.0	15.9	0.6	15	15	16	15	16	16
Total vertebrae	33.0	36.0	34.5	0.8	32	33	34	33	34	34
Vertebrae between first pterygiophores of dorsal and anal fins	9.0	11.0	9.8	0.7	10	10	11	10	11	11
Number of total lateral-line scales	10.0	34.0	23.9	7.5	0	7	0	0	0	0

Predorsal back outline markedly rising and going parallel to ventral profile or sloping to dorsal-fin origin. Thus, body deepest in front of dorsal-fin origin. Pelvic fin origin below middle of dorsal-fin base. Caudal peduncle moderately deep (11–13% SL) and its depth varying within wide range of 55–69% of caudal-peduncle length. Head not deep (head depth at nape 53–60% HL), its length (24–26% SL) considerably exceeding maximum body depth (18–22% SL). Snout variably elongated, markedly arched in dorsal or ventral (Fig. 11a–e) view; neither transverse groove nor transverse lobe developed. Anterior extremity of ethmoid field (proboscis) slightly to markedly (Fig. 10c) elevated from rostral.

Eye absent; no eye fossa in examined specimens. Gular disc (Fig. 11a–e) well-developed in all specimens examined, slightly wider than long or disc length almost equal to disc width, with posterior margin considerably variable, truncate (Fig. 11e), roundish (Fig. 11a, c) or attenuated (Fig. 11b, d). Width of pulvinus about equal to disc length. Maximum width of mouth considerably exceeding disc length. Mouth inferior, mouth cleft clearly arched. Small papillae on torus, labellum and labrum. Rostral cap moderately wide, not completely covering upper lip and upper jaw (Fig. 11a–e), with markedly arched (in ventral aspect) slightly fimbriate distal margin. Anterior barbel shorter than posterior barbel.

Dorsal fin with 2 or 3 (found in 2 specimens only) unbranched and 7½ branched rays, anal fin with 2 unbranched and 5½ branched rays. Pectoral fin with 1 unbranched ray and 11 (3), 12 (7), 13 (3), or 14 (1) branched rays. Pelvic fin with single unbranched ray and 6–8 branched rays.

Body naked except for lateral line and (in three specimens) few (1–6) scattered scales behind opercule or further caudad right above or below lateral line. Lateral line

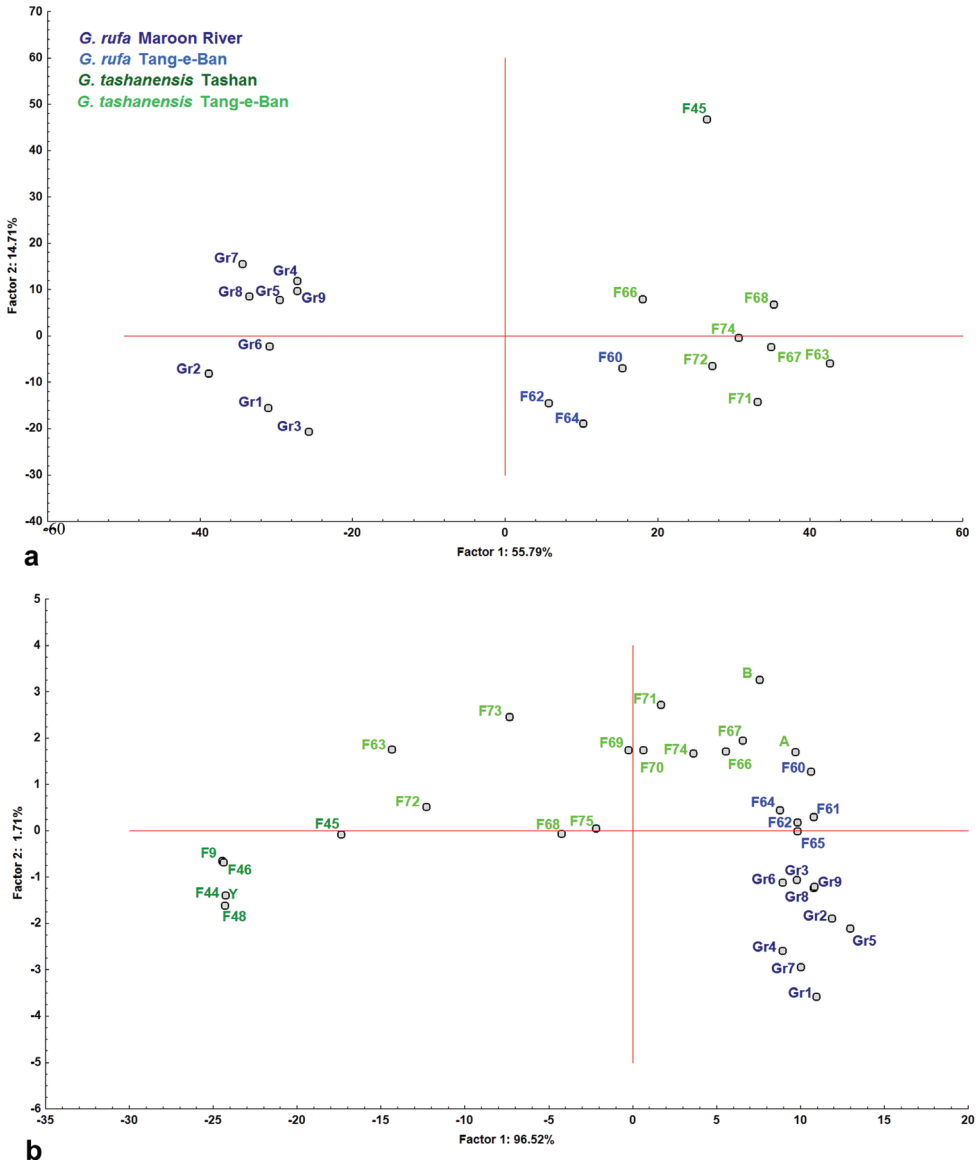

Figure 8. Results of PCA: using morphometric and meristic characters (total of 20 specimens) (**a**); using only meristic characters (total of 33 specimens) (**b**).

present in all examined specimens, variably shortened and interrupted, but commonly long or almost complete (in one specimen), with 10–34 (averaging 24) scales. Cephalic sensory canals complete, fully developed, non-interrupted.

Total vertebrae 33 (1), 34 (6), 35(5) or 36 (1); abdominal vertebrae 18(6) or 19 (7); predorsal abdominal vertebrae 11 (4), 12 (7) or 13 (1); caudal vertebrae 15(3), 16(8) or 17 (2); pre-anal caudal vertebrae 3 (4 in single specimen), post-anal caudal

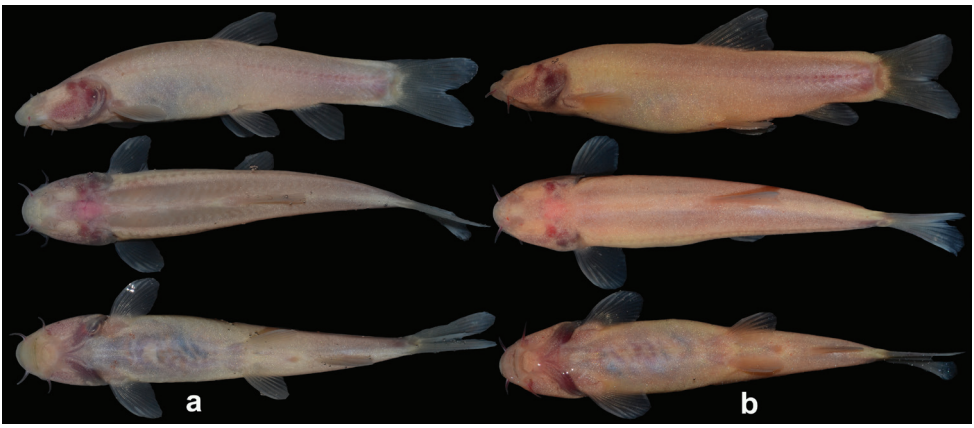

Figure 9. *Garra tashanensis*, Tang-e-Ban Spring, 20.04.2022, before preservation (just anesthetized), left lateral, dorsal and ventral views: F63, SL 43.3 mm (**a**); F66, SL 45.9 mm (**b**).

vertebrae 12 (4), 13 (7) or 14 (2); and 9(5), 10(6) or 11(2) vertebrae between first pterygiophores of dorsal and anal fins.

Body and fins unpigmented; in live specimens (Fig. 9) body is pinkish because of blood vessels seen through the semi-transparent skin. In preserved specimens, body is yellowish-white.

Description of the Tashan (type locality) disc-bearing phenotype

Measurements of one larger specimen and counts for all examined specimens are given in Tables 4, 5.

Longest examined specimen 42.2 mm SL (Fig. 10d). Body deep, thick; dorsal head profile slightly convex, its transition to back smooth, slight nuchal hump only in longest specimen. Predorsal back outline rising gently, slightly convex, to dorsal-fin origin. Pelvic-fin origin below middle of dorsal-fin base or slightly behind. Caudal peduncle deep and short, its depth varying within wide range of 80% of caudal-peduncle length. Head large (head length 28% SL) slightly exceeding maximum body depth (24% SL). Head wide and relatively deep; (head depth at nape 65% HL). Snout blunt and smooth; neither transverse groove nor transverse lobe developed. Anterior extremity of ethmoid field (proboscis) slightly elevated from rostral surface only in the longest specimen.

Eye absent; no eye fossae in examined specimens. Gular disc well-developed in all specimens examined (including smallest ones, SL 22.5–26 mm), wider than long (Fig. 11f), with roundish posterior margin. Width of pulvinus less than disc length. Maximum width of mouth considerably exceeding disc length. Mouth inferior, mouth cleft clearly straight. Small papillae on torus, labellum, and labrum. Rostral cap wide, completely covering upper lip and upper jaw (Fig. 11f), with almost straight (in ventral aspect) considerably fimbriate distal margin. Anterior barbel longer than posterior barbel. Dorsal fin with 3 unbranched and 7½ branched rays, anal fin with 2

Figure 10. *Garra tashanensis*, left lateral view: F67, SL 41.4 mm (**a**); F68, SL 39.5 mm (**b**); F72, SL 41.6 mm (**c**); and F45, SL 42.2 mm (**d**). Tang-e-Ban Spring, 20.04.2022 (**a–c**) and Tashan Cave (type-locality), 17.03.2018 (**d**).

unbranched and 5½ branched rays. Pectoral fin with 1 unbranched ray and 13(3) or 14(3) branched rays. Pelvic fin with single unbranched ray and 7 branched rays.

Body naked. Lateral line absent (in specimen up to SL 34.8 mm) or present by 7 segments behind head (in longest examined specimen of SL 42.2. mm). Cephalic sensory canals complete, fully developed, non-interrupted. Total vertebrae 32 (1), 33(2), or 34 (3); abdominal vertebrae 17(1) or 18 (5); predorsal abdominal vertebrae 10; caudal vertebrae 15(3) or 16(3); pre-anal caudal vertebrae 2(2) or 3 (4), post-anal caudal vertebrae 12 (1) or 13 (5); and 10(3) or 11 (3) vertebrae between first pterygiophores of dorsal and anal fins.

Body and fins unpigmented; in live specimens, body is pinkish because of blood vessels seen through the semi-transparent skin. In preserved specimens, body is yellowish-white.

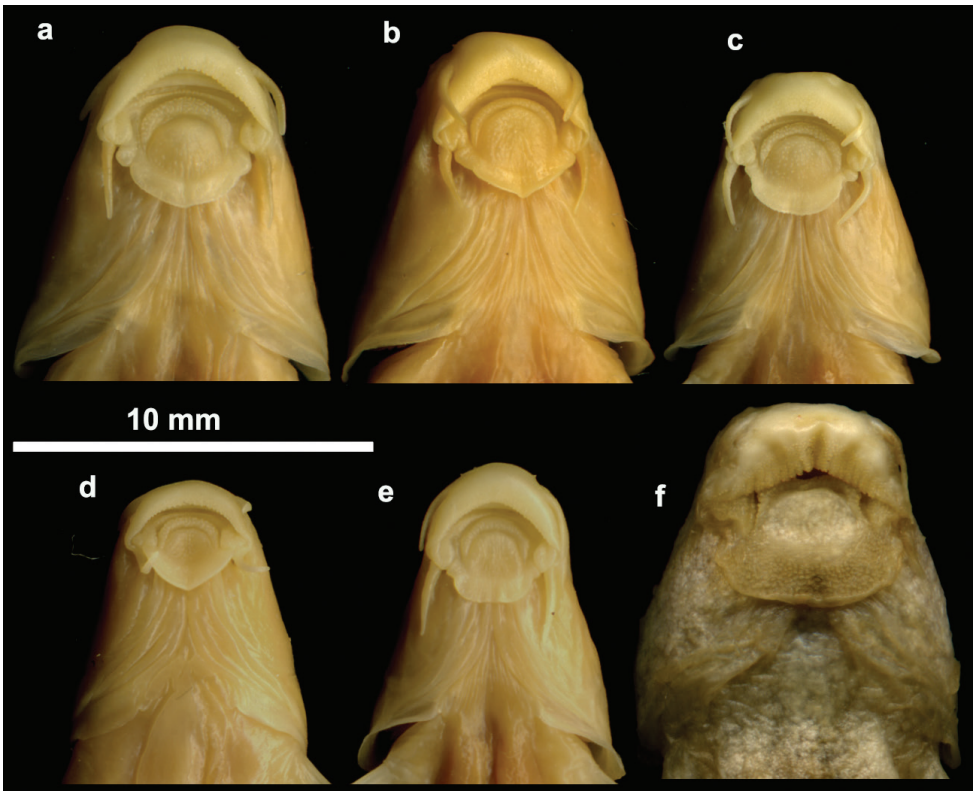

Figure 11. *Garra tashanensis*, head, ventral view: F73, SL 34.8 mm (**a**); F74, SL 40.1 mm (**b**); F75, SL 34.6 mm (**c**), specimen A, SL 33.9 mm (**d**); specimen B, SL 33.1 mm (**e**); and F45, SL 42.2 mm (**f**). Tang-e-Ban Spring, 20.04.2022 (**a–c**) and Tashan Cave (type-locality), 17.03.2018 (**d**).

Comparison between Tashan and Tang-e-Ban samples

As the lengths of two specimens in the Tashan sample were similar to those in most specimens in the Tang-e-Ban sample, we could suppose that differences were not size-dependent. On the other hand, the length of the smaller examined Tashan specimens (SL 22.5–26 mm) corresponds to the size of the holotype and paratypes of the species (SL 22–27 mm) (Mousavi-Sabet et al. 2016). In general, our study was consistent with the original description (Mousavi-Sabet et al. 2016: 136–139), except for the presence of a lateral line (7 pores) in the longer specimen (SL 42.2 mm). Hence, the absence of the lateral line cannot be considered a diagnostic feature of the species, as has been accepted (Zamani Faradonde et al. 2020a, b; Zamani Faradonde and Keyvani 2021) since the description of the species.

A comparison of the samples examined in the present study revealed some clear differences between them. Among the morphometric parameters, the most significant differences (results of the statistical analyses are presented below) are found in the following relative measurements (Table 4) (Tang-e-Ban vs. Tashan): maximum body

depth (18–22% SL vs. 24); depth of caudal peduncle (55–69% of caudal peduncle length vs. 80); caudal-peduncle length (18–21% SL vs. 15); body width (14–17% SL vs. 20); pectoral-fin length (17–19% SL vs. 21); head length (25–26% SL vs. 28); head depth at nape (54–60% HL vs. 65); anus – anal-fin origin distance (23–33% pelvic – anal-fin origin distance vs. 19); mouth width (37–45% HL vs. 51); disc width (30–35% HL vs. 44); disc length (91–99% disc width vs. 71); and pulvinus width (25–33% HL vs. 14).

Among the examined morphometric characters, the most prominent differences are commonly 2 unbranched dorsal-fin rays in the Tang-e-Ban sample (vs. 3 in the Tashan sample); commonly 11–12 branched pectoral-fin rays (vs. 13–14); 11–13 predorsal abdominal vertebrae (vs. 10); commonly 9–10 vertebrae between first pterygiophores of dorsal and anal fins (vs. 10–11); arched mouth cleft (vs. straitened), and, the most striking difference, well-developed lateral-line, with 10–34 pored scales imbedded into skin or externally visible (vs. up to maximum of 7 pores without visible scales).

The Tang-e-Ban and Tashan disc-bearing *G. tashanensis* samples are clustered in distinct groups in the CA (Fig. 7a). The PCA implemented using a combination of morphometric and meristic characters (Fig. 8a) show that the F65 specimen is clearly distant from the Tang-e-Ban. Interestingly, in the CA, the hypogean *G. rufa* sample was clustered together with the syntopic *G. tashanensis*, but not with epigean *G. rufa* occurring nearby. When only meristic characters were used, then the two groups were much closer in the PCA (Fig. 7b) and, in CA (Fig. 8b), even clustered together with one specimen of epigean *G. rufa* and one specimen of Tang-e-Ban *G. tashanensis.* In general, the examined specimens of disc-bearing *G. tashanensis* from Tang-e-Ban Spring are very morphologically heterogenous.

Discussion

In this study we reported a cave form of *G. rufa* currently known only from Tang-e-Ban spring (Figs 1, 2), thus, placing this population of the species in this karstic spring into the category of stygobionts. The other species that inhabits Tang-e-Ban spring is genetically clustered with stygobiotic *G. tashanensis*, a species previously known only from Tashan Cave. Our study thus adds a new form of stygobiont fish to complement the taxonomic understanding of the subterranean diversity of Iran. In total, five cave fish species of two genera from two families are now reported from Iran: four species of the genus *Garra* occur in groundwaters of Zagros Mountains, and *Eidinemacheilus smithi* is present in sympatry with two *Garra* species (*Garra lorestanensis* and *G. typhlops*) in Loven cave and Tuveh spring (which are 30 km apart) (Mousavi-Sabet et al. 2016; Malek-Hosseini and Zamani 2017; Malek-Hosseini et al. 2022).

The morphological analysis revealed that, although barcoded as *G. rufa* and *G. tashanensis*, the forms of these species inhabiting Tang-e-Ban significantly differ from the paired forms from the geographically very close Maroon River and Tashan Cave, respectively. As described above, the hypogean *G. rufa* from the Tang-e-Ban

spring differs from the conspecific epigean sample from the Maroon River by a variable level of loss of scales (except for the lateral line, which is complete); a continuum of eye reduction (up to a complete loss of externally visible eye structures); 7½ branched dorsal-fin, and a more anterior position of the anal fin relative to the pelvic fin, and a shorter distance between origins of the dorsal and anal fins (expressed both in external measurements and vertebral counts). The Tang-e-Ban *G. tashanensis* mostly differs from the type-bearing phenotype from Tashan cave in the body shape expressed in many relative measurements, commonly 2 unbranched dorsal-fins; a narrower disc; an arched mouth; and, the most striking difference, a well-developed lateral-line, with 10–34 pored scales imbedded into skin or externally visible (vs. up to maximum of 7 pores without visible scales). Morphological diversity of *G. tashanensis* is even higher as there is one more phenotype, a discless form, that occurs in syntopy with the disc-bearing phenotype in Tashan Cave (Hashemzadeh Segherloo et al. 2022; our data).

To distinguish between species, both morphological and genetic criteria should ideally be considered (Bond et al. 2022). Here, the K2P pairwise distance data between population of *Garra rufa* from Tang-e-Ban Spring and other localities was not sufficient to warrant description of a new species, despite the fact that different divergence rates have been applied as decisive criteria for new species (Ward et al. 2009; Esmaeili et al. 2016). This was similar for *G. tashanensis* from Tang-e-Ban Spring and Tashan Cave. These populations of *Garra* from Tang-e-Ban Spring, Tashan cave, Sarjowahar Spring, Maroon River, and also what we obtained from the literature, were conspecific with *G. rufa* and *G. tashanensis*, although some morphological differences and also genetic distances from 0.15% to 1.09% in barcoding COI gene were detected. We consider these as morphotypes of the same species resulting from environmental differences and/or prolonged isolation.

Our phylogenetic results were congruent with previous studies by Esmaeili et al. 2016, Kirchner et al. 2020 and Mousavi-Sabet et al. 2016. Phylogenetic studies based on a fragment of the COI gene (Kirchner et al. 2020) have revealed a close relationship of *Garra rufa* with a number of species, *G. persica* (Iran), *G. widdowsoni* (cave species from Iraq), *G. mondica* Sayyadzadeh (Iran), *G. amirhosseini*, *G. elegans* (Iran), *G. barreimiae* (UAE), *G. ghorensis* (Jordan), *G. jordanica* (Syria and Jordan), *G. typhlops*, *G. gymnothorax*, *G. lorestanensis* (Iran), and *G. longipinnis* (Oman). The sister group of this large clade is *G. tashanensis*. More markers from the abovementioned taxa and also other Iranian *Garra* species must be included in such studies to gain wider insights into the phylogenetic relationships of this group.

More studies are needed to examine the possibility of hybridisation between the two cave species occurring in Tang-e-Ban spring. Another question that will require genetic analyses is whether gene flow occurs between the epigean and hypogean morphotypes of *G. rufa*. We cannot exclude the possibility of existence of an epigean form of *G. tashanensis* in this area. A connection of Tashan cave with the Tang-e-Ban spring is also suggested by the occurrence of *G. tashanensis* in these two localities and may indicate the presence of an important aquifer in the Tashan area, consistent with unofficial reports by locals of "reddish-pinkish fishes" inhabiting other parts of the Tashan region.

Cave populations may remain interfertile with the ancestral surface form and, therefore, may not evolve into separate, reproductively isolated species, or subsequently they may split from the original epigean species following long isolation. Isolation of cave populations of *Garra* fishes can be quite old: for instance, the Somalian cave-dwelling species *Garra andruzzii* (Vinciguerra, 1924) became isolated about 5.3 Mya (at least 2.5 and at most 9.0 Mya; Calderoni et al. 2016), in contrast to *Astyanax mexicanus* where at least five independent events have led to cave-dwelling populations (still completely interfertile with the ancestral surface form) over the past 1–2 Mya (Bradic et al. 2012; Gross 2012).

As a result of old isolation, a diversity of situations is presently observed in *Garra*: there are some exclusively hypogean species such as *G. widdowsoni*, *G. lorestanensis*, and *G. typhlops* for which ancestral epigean forms remain unknown, whereas other species such as *G. longipinnis* and *G. barreimiae* include populations with both epigean and hypogean phenotypes (Banister 1984; Khalaf 2009; Kruckenhauser et al. 2011; Kirchner et al. 2017; Pichler et al. 2018; Kirchner et al. 2020; Freyhof et al. 2020; Sayyadzadeh et al. 2023). Further studies will be required to test the hypothesis that the latter situation corresponds to more recent cave colonisation events than the former.

Tang-e-Ban is a seasonal spring that flows during the period of February to June in highly rainy years. The spring is completely dry during the whole year with low precipitation and also from July until February-March in high-precipitation years. Several outflows for this spring exist, and it is not clear from which part fishes wash out. There are several springs close to Tang-e-Ban whose waters join together through agriculture lands with irrigation. Fish specimens either die in the spring or enter streams and the river. The whole area of Tashan will require comprehensive fieldwork and study to elucidate these mechanisms.

Our discovery of cave fishes in the Tashan area, as well as the presence of other troglobiotic/stygobiotic animals in Tashan cave (including a gastropod and an isopod) (Khalaji-Pirbalouty et al. 2018; Fatemi et al. 2019) reveal that this area should be considered a unique habitat that is worthy of urgent conservation, as numerous threats such as pollutants from human waste, water extraction, fish collection by locals, and uncontrolled human visits are putting the conservation of this unique habitat in danger.

Acknowledgements

Our sincere thanks go to Ernst Mikschi, Anja Palandačić, and all other members of the NHM Wien Fish Collection for their valuable help in studying the materials under their care. We are grateful to Mr. Barooninejad from Sarjowshar Village for his help and hospitality during sampling from Sarjowshar Spring. A language check of an earlier draft of the MS was carried out by Matthew Copley. Matjaž Kuntner was supported by the Slovenian Research and Innovation Agency (grant P1-0255). Jean-François Flot was supported by the Fonds de la Recherche Scientifique (F.R.S.-FNRS) via PDR grant T.0078.23.

References

Banister KE (1984) A subterranean population of *Garra barreimiae* (Teleostei: Cyprinidae) from Oman, with comments on the concept of regressive evolution. Journal of Natural History 18: 927–938. https://doi.org/10.1080/00222938400770811

Barr TC (1968) Cave ecology and the evolution of troglobites. In: Dobzhansky T, Hecht MK, Steere WC (Eds) Evolutionary Biology. New York, Appleton-Century-Crofts, 35–102. https://doi.org/10.1007/978-1-4684-8094-8_2

Bilandžija H, Abraham L, Ma L, Renner KJ, Jeffery WR (2018) Behavioural changes controlled by catecholaminergic systems explain recurrent loss of pigmentation in cavefish. Proceedings of the Royal Society B: Biological Sciences 285: 20180243. https://doi.org/10.1098/rspb.2018.0243

Bilandžija H, Hollifield B, Steck M, Meng G, Ng M, Koch AD, Gračan R, Ćetković H, Porter ML, Renner KJ, Jeffery W (2020) Phenotypic plasticity as a mechanism of cave colonization and adaptation. ELife 9: e51830. https://doi.org/10.7554/eLife.51830

Bond JE, Godwin RL, Colby JD, Newton LG, Zahnle XJ, Agnarsson I, Hamilton CA, Kuntner M (2022) Improving taxonomic practices and enhancing its extensibility–an example from araneology. Diversity 14(1): 5. https://doi.org/10.3390/d14010005

Borko Š, Trontelj P, Seehausen O, Moškrič A, Fišer C (2021) A subterranean adaptive radiation of amphipods in Europe. Nature Communications 12(1): 3688. https://doi.org/10.1038/s41467-021-24023-w

Bradic M, Beerli P, Garcıa de Leon FJ, Esquivel Bobadilla S, Borowsky RL (2012) Gene flow and population structure in the Mexican blind cavefish complex (*Astyanax mexicanus*). BMC Evolutionary Biology 12: 9. https://doi.org/10.1186/1471-2148-12-9

Calderoni L, Rota-Stabelli O, Frigato E, Panziera A, Kirchner S, Foulkes NS, Kruckenhauser L, Bertolucci C, Fuselli S (2016) Relaxed selective constraints drove functional modifications in peripheral photoreception of the cavefish *P. andruzzii* and provide insight into the time of cave colonization. Heredity 117: 383–392. https://doi.org/10.1038/hdy.2016.59

Christiansen KA (1962) Proposition pour la classification des animaux cavernicoles. Spelunca 2: 76–78.

Christiansen KA (2012) Morphological adaptations. In: White WB, Culver DC (Eds) Encyclopedia of Caves, 2nd edn. Academic/Elsevier Press, Amsterdam, 517–528. https://doi.org/10.1016/B978-0-12-383832-2.00075-X

Culver DC, Trontelj P, Zagmajster M, Pipan T (2013) Paving the way for standardized and comparable subterranean biodiversity studies. Subterranean Biology 10: 43–50. https://doi.org/10.3897/subtbiol.10.4759

Culver DC, Pipan T (2019) The Biology of Caves and Other Subterranean Habitats, 2nd edn., Biology of Habitats Series, Oxford. https://doi.org/10.1093/oso/9780198820765.001.0001

Culver DC, Deharveng L, Pipan T, Bedos A (2021) An overview of subterranean biodiversity hotspots. Diversity 13(10): 487. https://doi.org/10.3390/d13100487

Dudich E (1932) Biologie der Aggteleker Tropfsteinhöhle, "Baradla" in Ungarn. Speläologische Monographien, 13. Vienna, Verlag Speleologisches Institut Wien.

Esmaeili HR, Sayyadzadeh G, Coad B W, Eagderi S (2016) Review of the genus *Garra* hamilton, 1822 in Iran with description of a new species: a morpho-molecular approach (Teleostei: Cyprinidae). Iranian Journal of Ichthyology 3(2): 82–121.

Esmaeili HR, Mehraban H, Abbasi K, Keivany Y, Coad B (2017) Review and updated checklist of freshwater fishes of Iran: taxonomy, distribution and conservation status. Iranian Journal of Ichthyology 4(Suppl. 1): 1–114.

Fatemi Y, Malek-Hosseini MJ, Falniowski A, Hofman S, Kuntner M, Grego J (2019) Description of a new genus and species as the first gastropod species from caves in Iran. Journal of Cave and Karst Studies 81: 233–243. https://doi.org/10.4311/2019LSC0105

Freyhof J, Els J, Feulner GR, Hamidan NA, Krupp F (2020) Freshwater fishes of the Arabian Peninsula. Motivate Media Group, Dubai, 1–272.

Ghalenoei M, Pazooki J, Abdoli A, Hassanzadeh Kiabi B, Golzarianpour K (2010) Morphometric and meristic study of *Garra rufa* populations in Tigris and Persian Gulf Basins. Iranian Journal of Fisheries Sciences 19(3): 107–118.

Gross JB (2012) The complex origin of *Astyanax* cavefish. BMC Evolutionary Biology 12: 105. https://doi.org/10.1186/1471-2148-12-105

Hamidan NA, Geiger MF, Freyhof J (2014) *Garra jordanica*, a new species from the Dead Sea basin with remarks on the relationship of *G. ghorensis*, *G. tibanica* and *G. rufa* (Teleostei: Cyprinidae). Ichthyological Exploration of Freshwaters 25(3): 223–236.

Hammer Ø, Harper DAT, Ryan, PD (2001) Paleontological statistics software package for education and data analysis. Palaeontologia Electronica 4(1/4): 1–9. http://palaeo-electronica.org/2001_1/past/issue1_01.htm

Hashemzadeh Segherloo I, Ghaedrahmati N, Freyhof J (2016) *Eidinemacheilus*, a new generic name for *Noemacheilus smithi* Greenwood (Teleostei; Nemacheilidae). Zootaxa 4147(4): 466–476. https://doi.org/10.11646/zootaxa.4147.4.7

Hashemzadeh Segherloo I, Najafi Chaloshtory S, Naser MD, Yasser AG, Tabatabaei SN, Piette-Lauziere G, Mashtizadeh A, Elmi A, Sedighi O, Changizi A, Hallerman E, Bernatchez L (2022) Sympatric morphotypes of the restricted-range Tashan Cave *Garra*: distinct species or a case of phenotypic plasticity? Environmental Biology of Fishes 105(9): 1251–1260. https://doi.org/10.1007/s10641-022-01329-2

Huelsenbeck JP, Ronquist F (2001) MRBAYES: Bayesian inference of phylogenetic trees. Bioinformatics 17: 754–755. https://doi.org/10.1093/bioinformatics/17.8.754

Jeffery WR (2001) Cavefish as a model system in evolutionary developmental biology. Developmental Biology 231: 1–12. https://doi.org/10.1006/dbio.2000.0121

Jeffery WR (2005) Adaptive evolution of eye degeneration in the Mexican blind cavefish. Journal of Heredity 96(3): 185–196. https://doi.org/10.1093/jhered/esi028

Jouladeh-Roudbar A, Ghanavi HR, Doadrio I (2020) Ichthyofauna from Iranian Freshwater: Annotated Checklist, Diagnosis, Taxonomy, Distribution and Conservation Assessment. Zoological Studies 59: 21. https://doi.org/10.6620/ZS.2020.59-21

Khalaji-Pirbalouty V, Fatemi Y, Malek-Hosseini MJ, Kuntner M (2018) A new species of *Stenasellus* Dollfus, 1897 from Iran, with a key to the western Asian species (Crustacea, Isopoda, Stenasellidae). ZooKeys 766: 39–50. https://doi.org/10.3897/zookeys.766.23239

Keivany Y, Nezamoleslami A, Dorafshan S, Eagderi E (2016) Length-weight and length-length relationshipsin populations of *Garra rufa* from different rivers and basins of Iran. International Journal of Aquatic Biology 3(6): 409–413. https://doi.org/10.22034/ijab.v3i6.6

Khalaf NABAT (2009) *Garra barreimiae wurayahi* Khalaf, 2009: a new blind cave fish subspecies from Wadi Al Wurayah pools, Emirate of Fujairah, United Arab Emirates. Gazelle: The Palestinian Biological Bulletin 90 (June): 1–15.

Kimura M (1980) A simple method for estimating evolutionary rates of base substitutions through the comparative studies of sequence evolution. Journal of Molecular Evolution 16: 111–120. https://doi.org/10.1007/BF01731581

Kirchner S, Sattmann H, Haring E, Plan L, Victor R, Kruckenhauser L (2017) Investigating gene flow between the blind cavefish *Garra barreimiae* and its conspecific surface populations. Scientific Reports 7: 5130. https://doi.org/10.1038/s41598-017-05194-3

Kirchner S, Kruckenhauser L, Pichler A, Borkenhagen K, Freyhof J (2020) Revision of the *Garra* species of the Hajar Mountains in Oman and the United Arab Emirates with the description of two new species (Teleostei: Cyprinidae). Zootaxa 4751(3): 521–545. https://doi.org/10.11646/zootaxa.4751.3.6

Kirchner S, Sattmann H, Haring E, Victor R, Kruckenhauser L (2021) Hidden diversity–Delimitation of cryptic species and phylogeography of the cyprinid *Garra* species complex in Northern Oman. Journal of Zoological Systematics and Evolutionary Research 59(2): 411–427. https://doi.org/10.1111/jzs.12438

Kottelat M (2020) *Ceratogarra*, a genus name for *Garra cambodgiensis* and *G. fasciacauda* and comments on the oral and gular soft anatomy in labeonine fishes (Teleostei: Cyprinidae). Raffles Bulletin of Zoology Suppl. 7600(35): 156–178.

Krishnan J, Rohner N (2016) Cavefish and the basis for eye loss. Philosophical Transactions of the Royal Society B: Biological Sciences 372(1713): 20150487. https://doi.org/10.1098/rstb.2015.0487

Kruckenhauser L, Haring E, Sattmann H (2011) Genetic differentiation between cave and surface-dwelling populations of *Garra barreimiae* (Cyprinidae) in Oman. BMC Evolutionary Biology 11: 172. https://doi.org/10.1186/1471-2148-11-172

Krupp F, Schneider W (1989) The fishes of the Jordan River drainage basin and Azraq Oasis. Fauna of Saudi Arabia 1: 347–416.

Kumar S, Stecher G, Li M, Knyaz C, Tamura K (2018) MEGA X: Molecular evolutionary genetics analysis across computing platforms. Molecular Biology and Evolution 35: 1547–1549. https://doi.org/10.1093/molbev/msy096

Maddison W, Maddison D (2018) Mesquite: A modular system for evolutionary analysis version, 570 pp. http://www.mesquiteproject.org

Malek-Hosseini MJ, Fatemi Y, Esmaeili HR, Lokovšek T, Kuntner M (2022) A new locality for the blind loach, *Eidinemacheilus smithi* (Teleostei: Nemacheilidae) in Iranian Zagros: a morpho-molecular approach. Diversity 14(9): 724. https://doi.org/10.3390/d14090724

Malek-Hosseini MJ, Zamani A (2017) A checklist of subterranean arthropods of Iran. Subterranean Biology 21: 19–46. https://doi.org/10.3897/subtbiol.21.10573

Minh BQ, Schmidt HA, Chernomor O, Schrempf D, Woodhams MD, von Haeseler A, Lanfear R, Teeling E (2020) IQ-TREE 2: New models and efficient methods for phylogenetic

inference in the genomic era. Molecular Biology and Evolution 37(5): 1530–1534. https://doi.org/10.1093/molbev/msaa015

Mousavi-Sabet H, Eagderi S (2016) *Garra lorestanensis*, a new cave fish from the Tigris River drainage with remarks on the subterranean fishes in Iran (Teleostei: Cyprinidae). FishTaxa 1(1): 45–54.

Mousavi-Sabet H, Vatandoust S, Fatemi Y, Eagderi S (2016) Tashan Cave a new cave fish locality for Iran; and *Garra tashanensis*, a new blind species from the Tigris River drainage (Teleostei: Cyprinidae). FishTaxa 1(3): 133–148.

Naseka AM (1996) Comparative study on the vertebral column in the Gobioninae (Cyprinidae, Pisces) with special reference to its systematics. Publicaciones Especiales del Instituto Espanol de Oceanografia 21: 149–167.

Nebeshwar K, Vishwanath W (2017) On the snout and oromandibular morphology of genus *Garra*, description of two new species from the Koladyne River basin in Mizoram, India, and redescription of *G. manipurensis* (Teleostei: Cyprinidae). Ichthyological Exploration of Freshwaters 28(1): 17–53.

Pavan M (1944) Considerazioni sui concetti di troglobio, troglofilo e troglosseno. Le Grotte d'Italia, ser 2, 5: 35–41.

Pichler A, Ahnelt H, Kirchner S, Sattmann H, Haring E, Handschuh S, Freyhof J, Victor R, Kruckenhauser L (2018) The morphological diversity of *Garra barreimiae* [Teleostei: Cyprinidae]. Environmental Biology of Fishes 101(6): 1053–1065. https://doi.org/10.1007/s10641-018-0758-7

Pipan T, Culver DC (2012) Convergence and divergence in the subterranean realm: A reassessment. In Biological Journal of the Linnean Society 107(1): 1–14. https://doi.org/10.1111/j.1095-8312.2012.01964.x

Proudlove GS (2023) Subterranean Fishes of the World. https://cavefishes.org.uk/ [accessed on 21 January 2023]

Rambaut A, Drummond AJ, Xie D, Baele G, Suchar MA (2018) Posterior summarization in Bayesian phylogenetics using Tracer 1.7. Systematic Biology 67(5): 901–904. https://doi.org/10.1093/sysbio/syy032

Romero A, Paulson KM (2001) It's a wonderful hypogean life: a guide to the troglomorphic fishes of the world. Environmental Biology of Fishes 62(1): 13–41. https://doi.org/10.1023/A:1011844404235

Ruffo S (1957) Le attuali conoscenze sulla fauna cavernicola della Regione Pugliese. Memorie di Biogeografia Adriatica 3: 1–143.

Sayyadzadeh G, Esmaeili HR, Freyhof J (2015) *Garra mondica*, a new species from the Mond River drainage with remarks on the genus *Garra* from the Persian Gulf basin in Iran (Teleostei: Cyprinidae). Zootaxa 4048(1): 75–89. https://doi.org/10.11646/zootaxa.4048.1.4

Sayyadzadeh G, Al Jufaili SM, Esmaeili HR (2023) Species diversity deflation: Insight into taxonomic validity of *Garra* species (Teleostei: Cyprinidae) from Dhofar Region in the Arabian Peninsula using an integrated morpho-molecular approach. Zootaxa 5230: 333–350. https://doi.org/10.11646/zootaxa.5230.3.4

Sket B (1985) Why all cave animals do not look alike – a discussion on adaptive value of reduction processes. Bulletin of the National Speleological Society 47: 78–85.

Sket B (1999) The nature of biodiversity in hypogean waters and how it is endangered. Biodiversity and Conservation 8: 1319–1338. https://doi.org/10.1023/A:1008916601121

Sket B (2004) Subterranean habitats. In: Gunn J (Ed.) Encyclopedia of cave and karst science. New York and London (UK): Fitzroy Dearborn, 709–713.

Sket B (2008) Can we agree on an ecological classification of subterranean animals? Journal of Natural History 42(21–22): 1549–1563. https://doi.org/10.1080/00222930801995762

Stemmer M, Schuhmacher LN, Foulkes NS, Bertolucci C, Wittbrodt J (2015) Cavefish eye loss in response to an early block in retinal differentiation progression. Development 142(4): 743–752. https://doi.org/10.1242/dev.114629

Trajano E, de Carvalho MR (2017) Towards a biologically meaningful classification of subterranean organisms: a critical analysis of the Schiner-Racovitza system from a historical perspective, difficulties of its application and implications for conservation. Subterranean Biology 22: 1–26. https://doi.org/10.3897/subtbiol.22.9759

Vatandoust S, Mousavi-Sabet H, Geiger MF, Freyhof J (2019) A new record of Iranian subterranean fishes reveals the potential presence of a large freshwater aquifer in the Zagros Mountains. Journal of Applied Ichthyology 35(6): 1269–1275. https://doi.org/10.1111/jai.13964

Ward RD, Zemlak TS, Innes HB, Last RP, Hebert PDN (2005) DNA barcoding Australia's fish species. Philosophical Transactions of the Royal Society of London, Series B, Biological Sciences 360(1462): 1847–1857. https://doi.org/10.1098/rstb.2005.1716

Ward RD, Hanner R, Hebert PDN (2009) The campaign to DNA barcode all fishes. Journal of Fish Biology 74: 329–356. https://doi.org/10.1111/j.1095-8649.2008.02080.x

Wilkens H (1988) Evolution and genetics of epigean and cave *Astyanax fasciatus* (Characidae, Pisces). Evolutionary Biology 23: 271–367. https://doi.org/10.1007/978-1-4613-1043-3_8

Wilkens H, Strecker U (2017) Evolution in the dark. Darwin's loss without selection. Springer, Berlin, 226 pp. https://doi.org/10.1007/978-3-662-54512-6

Yamamoto Y, Jeffery WR (2011) Bony fishes. Blind cavefish. In: Farrell AP (Ed.) Encyclopedia of fish physiology. Elsevier Academic, Amsterdam, 1843–1849. https://doi.org/10.1016/B978-0-12-374553-8.00245-8

Zagmajster M, Malard F, Eme E, Culver DC (2018) Subterranean biodiversity patterns from global to regional scales. In: Moldovan OT, Kováč L, Halse S (Eds) Cave Ecology. Cham, Switzerland: Springer, 195–225. https://doi.org/10.1023/A:1011844404235

Zamani-Faradonbe, M, Keivany Y, Dorafshan S, Abbasi-Jeshvaghani M (2020a) Body shape variation of *Garra rufa* (Heckel, 1843) (Teleostei: Cyprinidae) using geometric andmorphometric techniques. Journal of Animal Diversity 2(1): 127–140. https://doi.org/10.29252/JAD.2020.2.1.5

Zamani-Faradonbe M, Keivany Y, Abbasi-Jeshvaghani M, Asadi-Namavar M (2020b) Morphometric and meristic variation in twelve different populations of *Garra rufa* (Heckel, 1843) from Iran. Jordan Journal of Natural History 7: 108–124.

Zamani-Faradonbe M, Keivany Y (2021) Two new species of *Garra* (Teleostei: Cyprinidae) from western Iran. Ichthyological Exploration of Freshwaters 30(3): 249–270. http://doi.org/10.23788/IEF-1137

Supplementary material 1

GenBank accession numbers for COI (codes in bold are our original sequences)
Authors: Mohammad Javad Malek-Hosseini, Jean-François Flot, Yaser Fatemi, Hamid Baboli Moakher, Matjaž Kuntner, Oleg A. Diripasko, Dušan Jelić, Nina G. Bogutskaya
Data type: pdf

Link: https://doi.org/10.3897/subtbiol.46.108396.suppl1

Supplementary material 2

Alignment S1
Authors: Mohammad Javad Malek-Hosseini, Jean-François Flot, Yaser Fatemi, Hamid Baboli Moakher, Matjaž Kuntner, Oleg A. Diripasko, Dušan Jelić, Nina G. Bogutskaya
Data type: fas
Explanation note: Fasta file of COI sequences used in our analyses.

Link: https://doi.org/10.3897/subtbiol.46.108396.suppl2